T.C.
SÜLEYMAN DEMİREL UNIVERSITY
GRADUATE SCHOOL OF NATURAL AND APPLIED SCIENCES

NEUTRINO MASS GENERATION AS A PROBE OF NEW PHYSICS BEYOND THE STANDARD MODEL

Maladh Kamal Yaseen AL-ANSSARI

Supervisor
Assoc. Prof. Dr. Gaber FAISEL

THE DEGREE OF DOCTOR OF PHILOSOPHY
DEPARTMENT OF PHYSICS
ISPARTA – 2023

TABLE OF CONTENTS

Page

ABSTRACT

Ph.D. Thesis

NEUTRINO MASS GENERATION AS A PROBE OF NEW PHYSICS BEYOND THE STANDART MODEL

Maladh Kamal Yaseen AL-ANSSARI

Süleyman Demirel University
Graduate School of Natural and Applied Sciences
Department of Physics

Supervisor: Assoc. Prof. Dr. Gaber FAISEL

In this thesis we attempt to explore one of the mechanisms of generating neutrino mass in a proposed extension of the standard model known as the scotogenic model. Particularly, we consider the radiative neutrino mass generation mechanism. This mechanism is desirable as it generates naturally small neutrino masses favored by the experimental results obtained in the last few decays from several number of experiments and searches. The proposed study in this thesis is to examine the possibility of generating neutrino masses in the framework of the scotogenic model. In this model, neutrino masses can be generated radiatively through a one loop Feynman diagram with new particles associated with the model running in the loop. These new particles are the three singlet right handed fermions N_1, N_2 and N_3 and the scalar and pseudoscalar components of the extra Higgs doublet proposed in the scotogenic model. In this work, we investigate the parameter space of the scotogenic model that can lead to generation of neutrino masses of order eV which are favored by several experimental results related to neutrino mixing and oscillations. We show that there are possible ranges in the parameter space of the model where neutrino masses can be generated and be of order eV without violating the bounds obtained from several processes such as lepton flavor process, Dark Matter relic density measurements and other relevant bounds. The obtained parameter space will have impact on processes that can be searched at current and future particle colliders. So, it will be helpful to check this impact to shed more light on the scotogenic model. Studies that will be carried out in this proposed thesis can thus be used to discriminate between new physics models beyond the Standard Model that can generate neutrino masses.Our research shows that "new physics" is shorthand for theories and models that expand upon the Standard Model.Its try to account for phenomena like dark matter and neutrino mass creation that the standard model cannot.

Keywords: Standard Model, Neutrinos, New Physics

2023, 62 pages

ÖZET

Doktora Tezi

NÖTRINO KÜTLE ÜRETIMI ILE STANDART MODEL ÖTESI FIZIĞIN ARAŞTIRILMASI

Maladh Kamal Yaseen AL-ANSSARI

Süleyman Demirel Üniversitesi
Fen Bilimleri Enstitüsü
Fizk Anabilim Dalı

Danışman: Assoc. Prof. Dr. Gaber FAISEL

Bu tezde, skotojenik model olarak bilinen standart modelin önerilen bir uzantısında nötrino kütlesi üretme mekanizmalarından birini incelemeyi amaçlamaktayız. Özellikle,radyatif nötrino kütle üretim mekanizmasını ele almaktayız. Bu mekanizma, son birkaç parçalanmada çok sayıda deney ve araştırmadan elde edilen deneysel sonuçlar tarafından tercih edilen doğal olarak küçük nötrino kütleleri ürettiği için arzu edilmektedir. Bu tezdeki önerilen çalışma, skotojenik model çerçevesinde nötrino kütleleri üretme olasılığını incelemektir. Bu modelde, döngüde çalışan modelle ilişkili yeni parçacıklarla tek döngülü bir Feynman diyagramı aracılığıyla radyatif olarak nötrino kütleleri üretilebilir. Bu yeni parçacıklar, modeldeki döngüde yer alan üç adet singlet sağ yön fermiyonları N_1, N_2 ve N_3 ve skotojenik modelde önerilen ekstra Higgs çiftinin skaler ve pseudoskaler bileşenleridir. Bu çalışmada, nötrino karışımı ve salınımları ile ilgili çeşitli deneysel sonuçlar tarafından tercih edilen eV düzeyinde nötrino kütlelerinin üretilmesine yol açabilecek skotojenik modelin parametre boşluğunu araştırmaktayız. Modelin parametre boşluğunda, lepton özelliği süreci, Karanlık Madde kalıntı yoğunluğu ölçümleri ve diğer ilgili sınırlar gibi çeşitli süreçlerden elde edilen sınırları ihlal etmeden nötrino kütlelerinin üretilebileceği ve eV düzeyinde olabileceği olası aralıklar olduğunu göstermekteyiz. Elde edilen parametre boşluğu, mevcut ve gelecekteki parçacık çarpıştırıcılarında araştırılabilecek süreçler üzerinde etkili olacaktır. Bu nedenle, bu etkiyi kontrol etmek, skotojenik modeli daha iyi anlamamıza yardımcı olacaktır. Önerilen bu tezde yapılacak çalışmalar, böylece, Standart Modelin ötesinde, nötrino kütleleri üretebilen yeni fizik modelleri arasında ayrım yapmak için kullanılabilir. Bu hipotezler, standart modelin yapamadığı karanlık madde ve nötrino kütlesi oluşumu gibi fenomenleri açıklamaya çalışır.Eldeki bu sonuçla, elde edilen parametre için mevcut ve gelecekteki çarpıştırıcılarda test edilebilecek belirli süreçler için model tahminlerini kontrol etmek ilginçtir. .boşluk Bunu yapmak ve sonuçları standart model ve bu tür süreçlerin skotojenik model tahminleriyle karşılaştırmak, standart modelin ötesinde yeni fiziğe ışık tutabilir. Araştırmamız, "yeni fiziğin" Standart Model üzerinde genişleyen teoriler ve modeller için kısa olduğunu gösteriyor. Standart modelin yapamadığı karanlık madde ve nötrino kütle oluşumu gibi fenomenleri açıklama girişimi.

Anahtar Kelimeler: Standart Model, Nötrinolar, Yeni Fizik

2023, 62 sayfa

ACKNOWLEDGMENTS

I owe the greatest gratitude to God without whom none of this would have been possible, and I would like to take this time to express my gratitude to everyone who has helped me throughout my research, especially my advisor Dr. Gaber Faisel. I would like to thank everyone who made my time in the University's physics department so enjoyable and productive, as well as everyone else who helped me all the way with my dissertation. Finally thanks for the support and advice from my Family and friends, for which I am grateful.

Maladh Kamal Yaseen AL-ANSSARI
ISPARTA, 2023

LIST OF FIGURES

Page

LIST OF TABLES

Page

LIST OF SYMBOLS AND ABBREVIATION

CKM	Cabibbo-Kobayashi-Maskawa
DM	Dark matter
FCNC	Flavour changing neutral currents
ILC	International Linear Collider
KGF	Kolar Gold Fields
LHC	Large Hadron Collider
ON	Ordering Normal
PMNS	Pontecorvo-Maki-Nakagawa-Sakata
QCD	Quantum chromodynamics
SM	Standard Model
VEV	Vacuum expectation value VEV
ε	Total Energy density
m_D	Dirac mass
m_R	Majorana mass

1. INTRODUCTION

This chapter summarizes neutrinos, which are the focus of this thesis study. We will start by giving a quick review of the neutrinos. Then we will discuss the research objective of this thesis and finally the structure of the thesis.

In the early 20th century, scientists were beginning to unravel the mysteries of the atom. One of the biggest questions was how energy was released during radioactive decays. In 1930, Wolfgang Pauli proposed that there must be a particle that carried away the missing energy, which he called the neutrino. It wasn't until 1956 that Clyde Cowan and Frederick Reines detected the neutrino experimentally, confirming Pauli's hypothesis.

Neutrinos are incredibly elusive particles that interact very weakly with matter. They have no electric charge and very little mass, making them difficult to detect. However, they are produced in large numbers by nuclear reactions in stars and in our own sun. By studying neutrinos, scientists can learn more about the inner working mechanisms of these celestial bodies and gain insights into the fundamental nature of matter itself.

The neutrino's flavor can change as it travels over space, a phenomenon known as neutrino oscillation. Three sorts of neutrinos, or "flavors," account for this phenomenon. They may change flavors on the fly as they travel between locations. This process was first observed in the late 1990s and has since become an area of intense study in physics. Neutrino oscillation provides essential insights into the properties of these elusive particles and could have ramifications for how we conceptualize the physical world. Neutrinos once thought to be massless, have been discovered to have a little but non-zero masses. This discovery has opened up new avenues of research in particle physics and astrophysics, leading to exciting breakthroughs in our understanding of the universe.

Current research on neutrinos is focused on studying their properties and behavior, including their interactions with other particles and their role in the formation and evolution of galaxies. Scientists are also exploring potential applications of neutrinos, such as using them for communication or detecting hidden nuclear materials.

These tiny particles are produced in abundance by stars and supernovae, and their detection has provided valuable insights into the sources producing them.
One of the most fascinating aspects of neutrinos in astrophysics is their ability to travel vast distances without being affected by electromagnetic forces. This makes them ideal messengers for studying objects in the universe that are the farthest away and have the most energy, such as black holes and gamma-ray bursts. By detecting these elusive particles, scientists can better understand the universe's composition and evolution.

1.1. Research Objective

Since it provides the most satisfactory explanations for the data gathered up to now, the Standard Model (SM) is now The majority prominent accepted model in particle physics. However, physicists maintain that this must be merely an active low energy realization of a basic theory. Experiments have provided several hints that lend credence to this notion. Neutrino oscillations are one example of such a suggestion; they point to the existence of a neutrino mass that is not zero, which runs counter to the predictions of the Standard Model.

This thesis attempts to uncover prospective candidates for innovative physics theories that go beyond the standard model by analyzing one of the proposed mechanisms for generating neutrino masses. Particularly, we consider an approach for generating neutrino masses known as the radiative neutrino mass generation. The novel physics models that make it possible are referred to as radiative neutrino mass models. These models are desirable because they naturally produce neutrino

masses with low masses. Favored by experimental results. The proposed investigation in this thesis will examine the possibility of generating neutrino masses in the framework of the scotogenic model. In this model, neutrino masses can be generated radiatively through a one loop Feynman diagram with new particles associated with the model running in the loop. These new particles are the three singlet right handed fermions N_1, N_2 and N_3 and the scalar and pseudoscalar components of the extra Higgs doublet proposed in the scotogenic model.

In our study, we will investigate the parameter space of the scotogenic model that can lead to generation of neutrino masses with values in the ranges favored by several experimental results related to neutrino mixing and oscillations. We will search for possible ranges in the parameter space of the model where neutrino masses can be generated and be of order eV without violating the bounds obtained from several processes such as lepton flavor process, relic density measurements and other relevant bounds as we will discuss in details in the following.

1.2. Thesis Structure

We briefly gave an overview about neutrinos in chapter one. In chapter two, the structure of the Standard Model (SM) will be presented. The mechanisms for generating neutrino masses will be discussed in chapter three. Chapter four will be devoted for the details about the structure of the scotogenic model and its particle content in addition to the relevant constraints that can be imposed on its parameter space. Then we show our analysis and results in chapter five. Finally, we will give our conclusion in chapter 6.

2. THE STANDARD MODEL

2.1. Gauge Group and Field Representations

The Standard Model (SM) is based on a symmetries represented by the product of the gauge groups (S. L. Glashow, 1961),

$$SU(3)_c \otimes SU(2)_L \otimes U(1)_Y \rightarrow SU(3)_c \otimes U(1)_Q \qquad (2.1)$$

here the Brout-Englert-Higgs mechanism suddenly breaks the electroweak symmetry to the electromagnetic symmetry. Three generations (families) of spin 1/2 fermions make up the matter in the SM, and a total of 8+3+1=12 gauge vector bosons mediate essential interactions (equal in number to generators of gauge groups). Particle masses are the result of the electroweak symmetry breaking triggered by the Higgs scalar field, of which one Higgs boson is a relic. The three types of fermions are listed in Table 2.1. Identical quarks or leptons (f and f') have different electric charges Q by one unit.

The SM is a chiral theory, with right and left-handed fermion field components residing in different gauge group representations. Strong and electroweak interactions have very different properties and can be studied separately.

$SU(3)_c$, is referred to as quantum chromodynamics (QCD) due to the fact that it is experienced solely as a result of particles with 'colour' charges, such as quarks (colour triplets), and gluons. The electroweak interactions (represented by the group $SU(2)_L \otimes U(1)_Y$) take into account the weak isospin and hypercharge (quantum flavor-dynamics) of fermions of any kind (or "flavour") of any type. The hypercharges of left-handed and right-handed fermions are distinct from one another, despite the fact that they are both isospin doublets. Quantum electrodynamics (QED) is the study of the relationship between electric charges Q

and the residual electroweak symmetry generator (the sum of the $SU(2)_L$ weak isospin T_3 and the $U(1)_Y$ hypercharge Y), which leads to quantum electrodynamics. Both right-handed and left-handed fermion fields have exactly the same gauge group representations for every quark and lepton family. The weak isospin of $SU(2)_L$, denoted by T_3, and the hypercharge of $U(1)_Y$, denoted by Y, are both functions that determine Q. Right-handed neutrinos, which are singlets and so sterile, were omitted from the early Standard Model, which only featured massless neutrinos.

Table 2.1. SM particle content (J.I.Illana and A.Jimenez Cano, 2022).

Fermions			1	2	3	4
Spin 1/2	Quarks	f	uuu	ccc	ttt	$\frac{2}{3}$
		f′	ddd	sss	bbb	$-\frac{1}{3}$
	Leptons	f	ν_e	ν_μ	ν_τ	0
		f′	e	μ	τ	-1

Bosons		accountable for
Spin(1)	gluons	strong interaction
	$W^{\pm}, Z$	weak interaction
	γ	em interaction
Spin(0)	Higgs	origin of mass

Table 2.2. Presentations of the left- and right-handed fermion fields in gauge groups (J.I.Illana and A.Jimenez Cano, 2022).

Multiplets	$SU(3)_c * SU(2)_L * U(1)_Y$	I	II	III	$Q = T_3 + Y$
Quarks	$\left(3, 2, \frac{1}{6}\right)$	$\begin{pmatrix} u_L \\ d_L \end{pmatrix}$	$\begin{pmatrix} c_L \\ s_L \end{pmatrix}$	$\begin{pmatrix} t_L \\ b_L \end{pmatrix}$	$\frac{2}{3} = \frac{1}{2} + \frac{1}{6}$ $-\frac{1}{3} = -\frac{1}{2} + \frac{1}{6}$
	$\left(3, 1, \frac{2}{3}\right)$	u_R	c_R	τ_R	$\frac{2}{3} = \frac{1}{2} + \frac{1}{6}$
	$\left(3, 1, -\frac{1}{3}\right)$	d_R	s_R	b_R	$-\frac{1}{3} = 0 - \frac{1}{3}$
Leptons	$\left(1, 2, -\frac{1}{2}\right)$	$\begin{pmatrix} u_{eL} \\ e_L \end{pmatrix}$	$\begin{pmatrix} u_{\mu L} \\ \mu_L \end{pmatrix}$	$\begin{pmatrix} u_{\tau L} \\ \tau_L \end{pmatrix}$	$0 = \frac{1}{2} - \frac{1}{2}$ $-1 = -\frac{1}{2} - \frac{1}{2}$
	$(1, 1, -1)$	eR	μR	τR	$-1 = 0 - 1$
	$(1, 1, 0)$	ν_{eR}	$\nu_{\mu R}$	$\nu_{\tau R}$	$0 = 0 + 0$

2.2. Electroweak Interactions

2.2.1. Gauge transformatıon of first family

Take the first family of massles fermions f (x) and f′(x) representing either quarks or leptons. We can express them in the $SU(2)_L \otimes U(1)_Y$ representations as

$$\Psi_1 = \begin{pmatrix} f_L \\ f'_L \end{pmatrix} \sim (2, y_1),\ \psi_2 = f_R \sim (1, y_2),\ \psi_3 = f'_R \sim (1, y_3), \tag{2.2}$$

And $P_{R,L} = \frac{1}{2}(1 \pm \gamma_5)f$ and $f_{R,L} = P_{R,L}f$ are the chiral projectors, and likewise for $f'_{R,L}$. Under global transformations and in the absence of potential energy,their Lagrangian is :

$$\mathcal{L}_F^0 = i\bar{f}\,\partial\!\!\!/ f + i\bar{f}'\,\partial\!\!\!/ f' = i\bar{\Psi}_1\,\partial\!\!\!/\Psi_1 + i\bar{\psi}_2\partial\!\!\!/\psi_2 + i\bar{\psi}_3\,\partial\!\!\!/\psi_3. \tag{2.3}$$

This Lagrangian ability to invariant under the following gauge transformations

$$\Psi_1(x) \ \mapsto U_L(x)e^{-iy_1\beta(x)}\Psi_1(x),\ U_L(x) = e^{-iT_i\alpha^i(x)},\ T_i = \frac{\sigma_i}{2} \tag{2.4}$$

$$\psi_2(x) \ \mapsto e^{-iy_2\beta(x)}\psi_2(x) \tag{2.5}$$

$$\psi_3(x) \ \mapsto e^{-iy_3\beta(x)}\psi_3(x), \tag{2.6}$$

Provided that substituting the covariant derivative for the derivative as

$$D_\mu\Psi_1 \ = \left(\partial_\mu - ig\widetilde{W}_\mu + ig'y_1B_\mu\right)\Psi_1,\ \widetilde{W}_\mu \equiv \frac{\sigma_i}{2}W_\mu^i, \tag{2.7}$$

$$D_\mu\psi_2 \ = \left(\partial_\mu + ig'y_2B_\mu\right)\psi_2, \tag{2.8}$$

$$D_\mu\psi_3 \ = \left(\partial_\mu + ig'y_3B_\mu\right)\psi_3, \tag{2.9}$$

where four gauge fields ($B_\mu(x)$ and $W_\mu^1(x), W_\mu^2(x), W_\mu^3(x)$) are along with two couplings (g and g′), one for every factor in a collection have been introduced as follow:

$$\widetilde{w}_\mu(x) \quad \mapsto U_L(x)\widetilde{w}_\mu(x)U_L^\dagger(x) - \frac{i}{g}\left(\partial_\mu u_L(x)\right)u_L^\dagger(x) \tag{2.10}$$

$$\widetilde{w}_\mu(x) \quad \to B_\mu(x) + \frac{1}{g'}\partial_\mu B(x). \tag{2.11}$$

Additionally, the Yang-Mills Lagrangian must be included.

$$\mathcal{L}_{YM} = -\tfrac{1}{4}W_{\mu\nu}^i W^{i,\mu\nu} - \tfrac{1}{4}B_{\mu\nu}B^{\mu\nu} \tag{2.12}$$

The two terms $B_{\mu\nu} = \partial_\mu B_\nu - \partial_\nu B_\mu$ and $W_{\mu\nu}^i = \partial_\mu W_\nu^i - \partial_\nu W_\mu^i + g\epsilon_{ijk}W_\mu^j W_\nu^k$ are self-interactions to gauge boson.

Under $SU(2)_L \otimes U(1)_Y$, the right and left-handed elements of the fermions can not change in the same method. Therefore, fermion Dirac masses given as

$$m\bar{f}f = m\left(\bar{f_L}f_R + \bar{f_R}f_L\right). \tag{2.13}$$

can not be symmetric under the gauge transformations and thus are not allowed. Charged current interactions, neutral current interactions, and gauge boson self-interactions are the three possible types of interactions and will be discussed in the following.

2.2.2. Charged current interactions

The term $g\bar{\Psi}_1\gamma^\mu\widetilde{W}_\mu\Psi_1$ in the interaction Lagrangian is not diagonal. To get the charged current interactions we define

$$\widetilde{W}_\mu = \frac{1}{2}\begin{pmatrix} W_\mu^3 & \sqrt{2}W_\mu^\dagger \\ \sqrt{2}W_\mu^- & -W_\mu^3 \end{pmatrix}, W_\mu^- \equiv \frac{1}{\sqrt{2}}\left(W_\mu^1 + iW_\mu^2\right), \quad W_\mu^+ \equiv \frac{1}{\sqrt{2}}\left(W_\mu^1 - iW_\mu^2\right) \quad (2.14)$$

This led to the charged current interaction Lagrangian expressed as

$$\mathcal{L}_{CC} = \frac{g}{\sqrt{2}}\bar{f}_L\gamma^\mu f_L' W_\mu^\dagger + \text{ h.c. } = \frac{g}{2\sqrt{2}}\bar{f}\gamma^\mu(1-\gamma_5)f' W_\mu^\dagger + \text{ h.c.} \quad (2.15)$$

Which can be represented diagramatically by

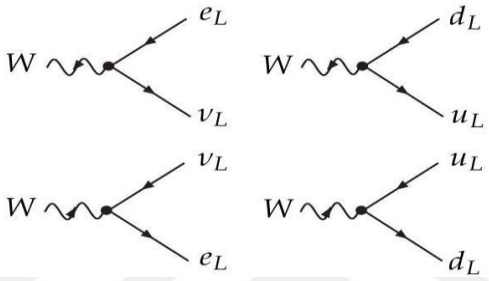

Figure 2.1. Weak charged current interactions (J.I.Illana and A.Jimenez Cano, 2022).

2.2.3. Neutral current interactions

Vector boson fields and their interactions (B_μ and W_μ^3) that do not affect the charge of fermions can be descibed by the diagonal part of $g\bar{\Psi}_1\gamma^\mu\widetilde{W}_\mu\Psi_1$ leading to the neutral current Lagrangian given as

$$\mathcal{L}_{NC} = \frac{1}{2}g\bar{\Psi}_1\gamma^\mu\sigma_3\Psi_1 W_\mu^3 - g'(y_1\bar{\Psi}_1\gamma^\mu\Psi_1 + y_2\bar{\psi}_2\gamma^\mu\psi_2 + y_3\bar{\psi}_3\gamma^\mu\psi_3)B_\mu, \quad (2.16)$$

Each fermion's chiralities must couple in a fashion that is directly related to its electric charge. In order to relate the gauge boson field B_μ only with the field representing the photons A_μ of QED we find that it is not possible because it would necessitate $g'y_j = eQ_j$ and $y_1 = y_2 = y_3$ at the same time. Since both B_μ and W_μ^3 are neutral, the following orthogonal combinations can be introduced:

$$\begin{pmatrix} W_\mu^3 \\ B_\mu \end{pmatrix} \equiv \begin{pmatrix} c_W & -s_W \\ s_W & c_W \end{pmatrix} \begin{pmatrix} Z_\mu \\ A_\mu \end{pmatrix},\ s_W \equiv \sin\theta_W\,,\ c_W \equiv \cos\theta_W, \tag{2.17}$$

where θ_W is the Weinberg angle (the weak mixing). Therefore, we can write the neutral current Lagrangian as

$$\mathcal{L}_{NC} = \sum_{j=1}^{3} \bar{\psi}_j \gamma^\mu \{-[gT_3 s_W + g' y_j c_W] A_\mu + [gT_3 c_W - g' y_j s_W] Z_\mu \} \psi_j \tag{2.18}$$

where $T_3 = \frac{1}{2}\sigma_3$ $(T_3 = 0)$ is the 3rd component of the isospin and $\psi_1 \equiv \Psi_1$ was proposed to simplify the Lagrangian. We have also the relations

$$e = g\, s_w = g' c_w,\ Q = T_3 + y. \tag{2.19}$$

which links electromagnetic couplings $e = g\, g'/\sqrt{g^2 + g'^2}$ to the couplings g of $SU(2)_L$ and g' of $U(1)_Y$. There are f and f' electric charges in the operators.

$$Q_1 = \begin{pmatrix} Q_f & 0 \\ 0 & Q_{f'} \end{pmatrix},\ Q_2 = Q_f,\ Q_3 = Q_{f'} \tag{2.20}$$

The weak isospin notation is used to express the hyperchanges as

$$y_1 = Q_f - \frac{1}{2} = Q_{f'} + \frac{1}{2},\ y_2 = Q_f,\ y_3 = Q_{f'}. \tag{2.21}$$

As a consequence, $\mathcal{L}_{NC} = \mathcal{L}_{QED} + \mathcal{L}_{NC}^{Z}$ includes the (γ) -mediated electromagnetic interactions

$$\mathcal{L}_{QED} = -e\, Q_f\, \bar{f}\, \gamma^\mu\, f\, A_\mu \ + (f \to f') \tag{2.22}$$

Moreover, $\mathcal{L}_{NC} = \mathcal{L}_{QED} + \mathcal{L}_{NC}^{Z}$ contains the Z boson field-mediated weak neutral current interactions.

$$\mathcal{L}_{NC}^{Z} = \; e\,\bar{f}\,\gamma^{\mu}\,(v_f - a_f\,\gamma_5)\,f\;Z_{\mu}\; + (f \to f') \tag{2.23}$$

with

$$v_f = \frac{T_3^{f_L} - 2\,Q_f\,s_W^2}{2\,s_W\,c_W},\;\; a_f = \frac{T_3^{f_L}}{2\,s_W\,c_W}, \tag{2.24}$$

where $T_3^{f_L}$ f_L corresponding eigenvalue in T_3. The v_R are sterile, while left-handed neutrinos v_L have only weak interactions, Consequently, missing from the initial SM of free of mass neutrino. f_L corresponding eigenvalue in T_3

(a) (b)

Figure 2.2. Interactions between neutral current and electromagnetic waves (J.I.Illana and A.Jimenez Cano, 2022).

2.2.4. Gauge boson self-interactions

The cubic interactions among the gauge boson fields can be listed as

$$\begin{aligned}\mathcal{L}_{YM} \supset \mathcal{L}_3 = \; & -\frac{iec_W}{s_W}\{W^{\mu\nu}W_{\mu}^{\dagger}Z_{\nu} - W_{\mu\nu}^{\dagger}W^{\mu}Z^{\nu} - W_{\mu}^{\dagger}W_{\nu}Z^{\mu\nu}\} \\ & +ie\{W^{\mu\nu}W_{\mu}^{\dagger}A_{\nu} - W_{\mu\nu}^{\dagger}W^{\mu}A^{\nu} - W_{\mu}^{\dagger}W_{\nu}F^{\mu\nu}\}\end{aligned} \tag{2.25}$$

with $F_{\mu\nu} = \partial_{\mu}A_{\nu} - \partial_{\nu}A_{\mu}, Z_{\mu\nu} = \partial_{\mu}Z_{\nu} - \partial_{\nu}Z_{\mu}, W_{\mu\nu} = \partial_{\mu}W_{\nu} - \partial_{\nu}W_{\mu}$. On the other hand, the quartic interactions of the gauge bosons are given as

$$
\begin{aligned}
\mathcal{L}_{YM} \supset \mathcal{L}_4 = \quad & -\frac{e^2}{2s_W^2}\left\{\left(W_\mu^\dagger W^\mu\right)^2 - W_\mu^\dagger W^{\mu\dagger} W_\nu W^\nu\right\} \\
& -\frac{e^2 c_W^2}{s_W^2}\left\{W_\mu^\dagger W^\mu Z_\nu Z^\nu - W_\mu^\dagger Z^\mu W_\nu Z^\nu\right\} \\
& +\frac{e^2 c_W}{s_W}\left\{2W_\mu^\dagger W^\mu Z_\nu A^\nu - W_\mu^\dagger Z^\mu W_\nu A^\nu - W_\mu^\dagger A^\mu W_\nu Z^\nu\right\} \\
& -e^2\left\{W_\mu^\dagger W^\mu A_\nu A^\nu - W_\mu^\dagger A^\mu W_\nu A^\nu\right\}.
\end{aligned}
\tag{2.26}
$$

There are an even number of W involved in the gauge boson self-interactions, and there is no vertex with only Z or γ. All the above mentioned gauge bosons interactions are shown in Fig. (2.3).

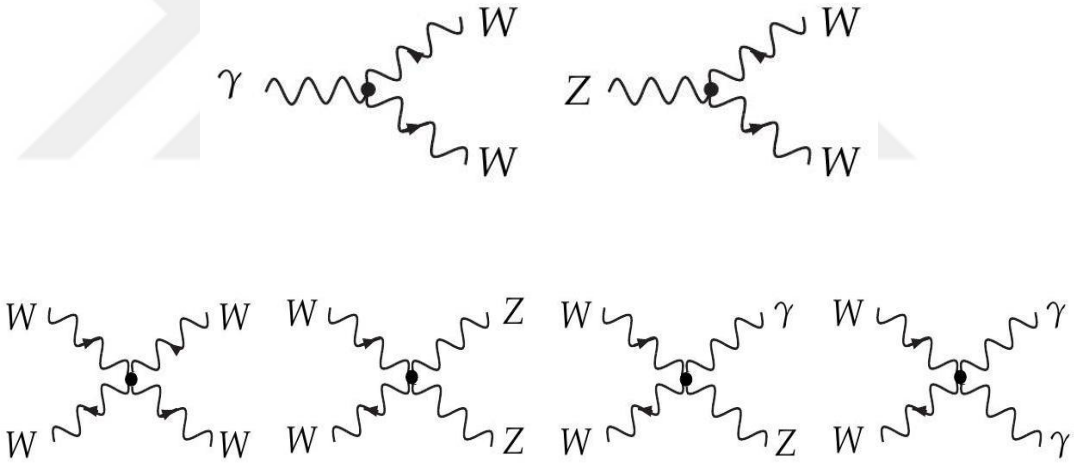

Figure 2.3. Triple and Quartic gauge boson interactions (J.I.Illana and A.Jimenez Cano, 2022).

2.3. Electroweak symmetry breaking: Higgs sector and gauge boson masses

The weak gauge bosons (Z and $W^{\pm}$) are massive particles. The Higgs mechanism is used to give Z and $W^{\pm}$ masses without directly violating gauge invariance It maintains the combination $Q = T_3 + Y$ unbroken and can not be carried out by introducing single complex scalar. It can be achieved by an SU(2) complex doublet of the Higgs boson with the right hypercharge, as shown below.

$$\Phi = \begin{pmatrix} \phi^+ \\ \phi^0 \end{pmatrix},\ \langle 0|\Phi|0\rangle \equiv \frac{1}{\sqrt{2}}\begin{pmatrix} 0 \\ v \end{pmatrix}, \tag{2.27}$$

With $v/\sqrt{2}$ is the minimum of the Mexican hat potential $V(\Phi)$, also known as the Higgs vacuum expectation value.

$$V(\Phi) = \mu^2\Phi^\dagger\Phi + \lambda(\Phi^\dagger\Phi)^2 \tag{2.28}$$

where, $\mu^2 = -\lambda v^2 < 0$.

The gauge invariance of the Higgs Lagrangian of the covariant derivative as:

$$\mathcal{L}_\Phi = \left(D_\mu\Phi\right)^\dagger D^\mu\Phi - V(\Phi),\ D_\mu\Phi = \left(\partial_\mu - ig\widetilde{W}_\mu + ig' y_\Phi B_\mu\right)\Phi. \tag{2.29}$$

Giving the Higgs doublet a hypercharge produces a vacuum-annihilating generator connected to the photon field and three others unrelated to the massive vector fields of $y_\Phi = \frac{1}{2}$, as follow:

$$(T_3 + Y)\begin{pmatrix} 0 \\ v \end{pmatrix} = 0 \text{ and } \{T_1, T_2, T_3 - Y\}\begin{pmatrix} 0 \\ v \end{pmatrix} \neq 0. \tag{2.30}$$

The gauge invariance of the unitary gauge allows for the absorption of the spacetime-dependent phases parameterized by the three hypothetical Goldstone fields in $\Phi(x)$.

$$\Phi(x) \equiv \exp\left\{i\frac{\sigma_i}{2v}\theta^i(x)\right\}\frac{1}{\sqrt{2}}\begin{pmatrix} 0 \\ v + H(x) \end{pmatrix} \mapsto \exp\left\{-i\frac{\sigma_i}{2v}\theta^i(x)\right\}\Phi(x)$$
$$= \frac{1}{\sqrt{2}}\begin{pmatrix} 0 \\ v + H(x) \end{pmatrix}. \tag{2.31}$$

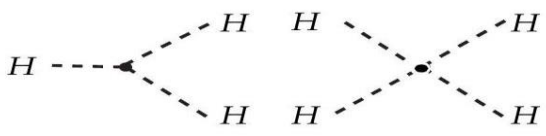

Figure 2.4. Higgs boson self-interactions (J.I.Illana and A.Jimenez Cano, 2022).

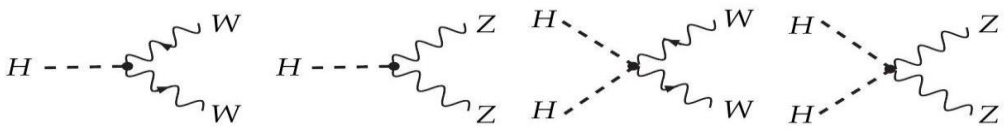

Figure 2.5. Higgs-gauge boson interactions (J.I.Illana and A.Jimenez Cano, 2022).

There is just one physical field which is the neutral Higgs field h(x). The extra three degrees of freedom become the longitudinal polarisation of $W^{\pm}$ and Z and hence their masses are given as:

$$\mathcal{L}_{\Phi} \supset \mathcal{L}_{M} = \frac{g^2 v^2}{4} W_{\mu}^{\dagger} W^{\mu} + \frac{g^2 v^2}{8 c_W^2} Z_{\mu} Z^{\mu} \Rightarrow M_W = M_Z c_W = \frac{1}{2} g v \tag{2.32}$$

The parameter $\rho \equiv M_W^2/(M_Z c_W)^2 = 1$ from data. The parameter ρ is used to determine the relative strenight of the neutral-current and charged-current (N. Cabibbo, 1963)

The unitary gauge Higgs Lagrangian is

$$\mathcal{L}_{\Phi} = \mathcal{L}_{H} + \mathcal{L}_{M} + \mathcal{L}_{HV} \tag{2.33}$$

$$\mathcal{L}_{H} = \frac{1}{2} \partial_{\mu} H \, \partial^{\mu} H - \frac{1}{2} M_H^2 H^2 - \frac{M_H^2}{2v} H^3 - \frac{M_H^2}{8v^2} H^4 \tag{2.34}$$

$$\mathcal{L}_{M} + \mathcal{L}_{HV} = M_W^2 W_{\mu}^{\dagger} W^{\mu} \left\{ 1 + \frac{2}{v} H + \frac{H^2}{v^2} \right\} + \frac{1}{2} M_Z^2 Z_{\mu} Z^{\mu} \left\{ 1 + \frac{2}{v} H + \frac{H^2}{v^2} \right\}, \tag{2.35}$$

where

$$M_H = \sqrt{-2\mu^2} = \sqrt{2\lambda} v. \tag{2.36}$$

The Higgs doublet can be parametrized as follow:

$$\Phi(x) \equiv \begin{pmatrix} \phi^+(x) \\ \frac{1}{\sqrt{2}}[v + H(x) + i\chi(x)] \end{pmatrix} \tag{2.37}$$

and $\phi^-(x) \equiv [\phi^+(x)]^\dagger$. Then the Higgs Lagrangian reads

$$\begin{aligned} \mathcal{L}_\Phi \quad &= \mathcal{L}_H + \mathcal{L}_M + \mathcal{L}_{HV^2} + (\partial_\mu \phi^+)(\partial^\mu \phi^-) + \frac{1}{2}(\partial_\mu \chi)(\partial^\mu \chi) \\ &\quad + iM_W\left(W_\mu\, \partial^\mu \phi^+ - W_\mu^\dagger\, \partial^\mu \phi^-\right) + M_Z Z_\mu\, \partial^\mu \chi \\ &\quad + \cdots \end{aligned} \tag{2.38}$$

Some of the neglected terms are those involving trilinear (SSS,SSV,SVV) and quadrilinear (SSS,SSV,SVV) interactions between vector (V) and scalar (S) fields and hypothetical Goldstone bosons.

A suitable gauge-fixing Lagrangian must be added for the purpose of defining propagators and doing away with cross words

$$W_\mu\, \partial^\mu \phi^+, W_\mu^\dagger\, \partial^\mu \phi^-, Z_\mu\, \partial^\mu \chi.$$

$$\begin{aligned} \mathcal{L}_{GF} = &-\frac{1}{2\xi_\gamma}\left(\partial_\mu A^\mu\right)^2 - \frac{1}{2\xi_Z}\left(\partial_\mu Z^\mu - \xi_Z M_Z \chi\right)^2 \\ &- \frac{1}{\xi_W}\left|\partial_\mu W^\mu + i\xi_W M_W \phi^-\right|^2. \end{aligned} \tag{2.39}$$

Following that, a massless photon propagator can be found. The propagators of the gauge bosons are given as:

$$\widetilde{D}_{\mu\nu}^{\gamma}(k) = \frac{i}{k^2 + i\varepsilon}\left[-g_{\mu\nu} + (1 - \xi_\gamma)\frac{k_\mu k_\nu}{k^2}\right]. \tag{2.40}$$

$$\widetilde{D}^{Z}_{\mu\nu}(k) = \frac{i}{k^2 - M_Z^2 + i\varepsilon}\left[-g_{\mu\nu} + (1-\xi_Z)\frac{k_\mu k_\nu}{k^2 - \xi_Z M_Z^2}\right];\ \widetilde{D}^{\chi}(k)$$

$$= \frac{i}{k^2 - \xi_Z M_Z^2 + i\varepsilon} \tag{2.41}$$

$$\widetilde{D}^{W}_{\mu\nu}(k) = \frac{i}{k^2 - M_W^2 + i\varepsilon}\left[-g_{\mu\nu} + (1-\xi_W)\frac{k_\mu k_\nu}{k^2 - \xi_W M_W^2}\right];\ \widetilde{D}^{\Phi}(k)$$

$$= \frac{i}{k^2 - \xi_W M_W^2 + i\varepsilon} \tag{2.42}$$

In the Feynman-'t Hooft gauge, these propagators are much simpler, the $\xi_\gamma = \xi_Z = \xi_W = 1$, is quite helpful when performing calculations using loops.

Since the electroweak symmetry group is non-Abelian, The theory operates at the quantum level. needs to have its gauge invariance fixed, and this can be done by including one Faddeev-Popov ghost for every SU(2) generator. They pair to the doublet of the Higgs boson in addition to the SU(2) gauge fields, following the EWSB.

$$\mathcal{L}_{FP} = (\partial^\mu \bar{c}_i)\left(\partial_\mu c_i - g\epsilon_{ijk} c_j W_\mu^k\right) + \text{ ghost interactions with } \Phi\,. \tag{2.43}$$

A series of the common weak and electromagnetic vector fields form the basis for the auxiliary fields $c_i(x)(i = 1,2,3)$

$$c_1 \equiv \frac{1}{\sqrt{2}}(u_+ + u_-),\ c_2 \equiv \frac{i}{\sqrt{2}}(u_+ - u_-),\ c_3 \equiv c_W u_Z - s_W u_\gamma. \tag{2.44}$$

We also provide the full Faddeev-Popov Lagrangian as follows:

$$
\begin{aligned}
\mathcal{L}_{FP} = \quad & (\partial_\mu \bar{u}_\gamma)(\partial^\mu u_\gamma) + (\partial_\mu \bar{u}_Z)(\partial^\mu u_Z) + (\partial_\mu \bar{u}_+)(\partial^\mu u_+) + (\partial_\mu \bar{u}_-)(\partial^\mu u_-) \\
& + ie[(\partial^\mu \bar{u}_+)u_+ - (\partial^\mu \bar{u}_-)u_-]A_\mu - \frac{iec_W}{s_W}[(\partial^\mu \bar{u}_+)u_+ - (\partial^\mu \bar{u}_-)u_-]Z_\mu \\
& - ie\left[(\partial^\mu \bar{u}_+)u_\gamma - (\partial^\mu \bar{u}_\gamma)u_-\right]W_\mu^\dagger + \frac{iec_W}{s_W}[(\partial^\mu \bar{u}_+)u_Z - (\partial^\mu \bar{u}_Z)u_-]W_\mu^\dagger \\
& + ie\left[(\partial^\mu \bar{u}_-)u_\gamma - (\partial^\mu \bar{u}_\gamma)u_+\right]W_\mu - \frac{iec_W}{s_W}[(\partial^\mu \bar{u}_-)u_Z - (\partial^\mu \bar{u}_Z)u_+]W_\mu \\
& - \xi_Z M_Z^2 \bar{u}_Z u_Z - \xi_W M_W^2 \bar{u}_+ u_+ - \xi_W M_W^2 \bar{u}_- u_- \\
& - e\xi_Z M_Z \bar{u}_Z \left[\frac{1}{2s_W c_W} H u_Z - \frac{1}{2s_W}(\phi^+ u_- + \phi^- u_+)\right] \\
& - e\xi_W M_W \bar{u}_+ \left[\frac{1}{2s_W}(H + i\chi)u_+ - \phi^+\left(u_\gamma - \frac{c_W^2 - s_W^2}{2s_W c_W} u_Z\right)\right] \\
& - e\xi_W M_W \bar{u}_- \left[\frac{1}{2s_W}(H - i\chi)u_- \right. \\
& \left. - \phi^-\left(u_\gamma - \frac{c_W^2 - s_W^2}{2s_W c_W} u_Z\right)\right] \qquad (2.45)
\end{aligned}
$$

In the Feynman Hooft gauge, the partner gauge boson fields have masses that are gauge-dependent, as shown by the kinetic terms.

$$
\begin{aligned}
& \tilde{D}^{u_\gamma}(k) = \frac{i}{k^2 + i\varepsilon}, \; \tilde{D}^{u_Z}(k) = \frac{i}{k^2 - \xi_Z M_Z^2 + i\varepsilon}, \; \tilde{D}^{u_\pm}(k) \\
& = \frac{i}{k^2 - \xi_W M_W^2 + i\varepsilon}. \qquad (2.46)
\end{aligned}
$$

2.4. Yukawa Interactions: Fermion Masses

Lepton and quark masses are also required, with maintaning gauge symmetry. To achieve this, a new interaction is created that couples the the Higgs doublet Φ and the fermion fields while maintaining the $SU(2)_L \otimes U(1)_Y$ symmetry. This is achievable using the following Yukawa interactions expressed in the following equation

$$\begin{aligned}\mathcal{L}_Y = &-\lambda_d(\bar{u}_L\ \bar{d}_L)\Phi d_R - \lambda_u(\bar{u}_L\ \bar{d}_L)\tilde{\Phi}u_R \\ &-\lambda_e(\bar{\nu}_L \quad \bar{e}_L)\Phi e_R - \lambda_\nu(\bar{\nu}_L \quad \bar{e}_L)\tilde{\Phi}\nu_R + \text{ h.c.},\end{aligned} \tag{2.47}$$

where $\tilde{\Phi} \equiv i\sigma_2\Phi^*$ contains the convenint quantum numbers. Under SU(2), $\tilde{\Phi}$ and Φ transforms similarly, although, $\tilde{\Phi}$ has opposite hypercharge than Φ.

In the first version of the SM, neutrinos had no mass. Hence their Yukawa couplings was not considered. Masses of fermions increase in accordance with their respective Yukawa couplings, as predicted by the EWSB.

$$\mathcal{L}_Y \supset -\frac{1}{\sqrt{2}}(v+H)\{\lambda_d\bar{d}d + \lambda_u\bar{u}u + \lambda_e\bar{e}e + \lambda_\nu\bar{\nu}\nu\} \Rightarrow m_f = \lambda_f\frac{v}{\sqrt{2}}, \tag{2.48}$$

recalling that $\bar{f}\,f = \bar{f_L}f_R + \bar{f_R}f_L$.

2.5. Fermion Mixings

Quarks and leptons have three generations. They are exact duplicates with the equivalent characteristics under $SU(2)_L \otimes U(1)_Y$. As it were thing that differentiates them is their masses. When one does n generations and specifies $u_i^I, d_i^I, \nu_i^I, e_i^I$ as the fields corresponding to the i-th generation, and the i standing for 'interaction' basis was neglected up until this point, an all-encompassing gauge-invariant Yukawa Lagrangian is as follows:

$$\mathcal{L}_Y = -\sum_{ij} \Big\{ (\bar{u}^I_{iL} \quad \bar{d}^I_{iL}) \Phi \lambda^{(d)}_{ij} d^I_{jR} + (\bar{u}^I_{iL} \quad \bar{d}^I_{iL}) \tilde{\Phi} \lambda^{(u)}_{ij} u^I_{jR} + (\bar{v}^I_{iL} \quad \bar{e}^I_{iL}) \Phi \lambda^{(e)}_{ij} e^I_{jR} + (\bar{v}^I_{iL} \quad \bar{e}^I_{iL}) \tilde{\Phi} \lambda^{(v)}_{ij} v^I_{jR} \Big\} + \text{h.c.} \tag{2.49}$$

Here $\lambda^{(d)}_{ij}, \lambda^{(u)}_{ij}, \lambda^{(e)}_{ij}$, and $\lambda^{(v)}_{ij}$. There exist n × n Yukawa matrices in flavour space. After the EWSB, this Lagrangian has a set of terms in the form of an n-dimensional matrix, as shown in Equation (2.50):

$$\mathcal{L}_Y \supset -\left(1 + \frac{H}{v}\right) \{ \bar{d}^I_L M_d d^I_R + \bar{u}^I_L M_u u^I_R + \bar{e}^I_L M_e e^I_R + \bar{v}^I_L M_v v^I_R + \text{ h.c. } \}, \tag{2.50}$$

using the form $(M_f)_{ij} = \lambda^{(f)}_{ij} v/\sqrt{2}$ for the matrices of different masses. In terms of interaction eigenfields d_j, u_j, e_j, v_j , and v^I_j the physical mass eigenfields d^I_j, u^I_j, $e^I_j, v^I_j$and v^I_j are determined, with v^I_j having a well-defined flavour. The formulas for each M_f are as follows:

$$M_f = H_f \mathcal{U}_f = V_f^\dagger \mathcal{M}_f V_f \mathcal{U}_f \Leftrightarrow \quad \Leftrightarrow \; M_f M_f^\dagger = H_f^2 = V_f^\dagger \mathcal{M}_f^2 V_f \tag{2.51}$$

with $H_f \equiv \sqrt{M_f M_f^\dagger}$ is a Hermitian positive definite matrix and $\mathcal{U}_f$ is a unitary matrix. H_f is being able to A unitary matrix V_f should be used to diagonalize with the outcome $\mathcal{M}_f$ is diagonal and positive definite. In the actual premise, the mass matrices are diagonal, $\mathcal{M}_d = \text{diag}(m_d, m_s, m_b, \dots)$, $\mathcal{M}_u = \text{diag}(m_u, m_c, m_t, \dots)$,and the $\mathcal{M}_e = \text{diag}(m_e, m_\mu, m_\tau, \dots), \mathcal{M}_v = \text{diag}\left(m_{v_e}, m_{v_\mu}, m_{v_\tau}, \dots\right)$. Fermion couplings to the Higgs are found to be proportional to fermion masses,

$$\mathcal{L}_Y \supset -\left(1 + \frac{H}{v}\right) \{ \bar{d} \mathcal{M}_d d + \bar{u} \mathcal{M}_u u + \bar{e} \mathcal{M}_e e + \bar{v} \mathcal{M}_v v \}. \tag{2.52}$$

Interaction with mass eigenfields is now being replaced as follow:

$$d_L \equiv V_d d_L^I,\ u_L \equiv V_u u_L^I,\ e_L \equiv V_e e_L^I,\ v_L \equiv V_v v_L^I \tag{2.53}$$

$$d_R \equiv V_d \mathcal{U}_d d_R^I,\ u_R \equiv V_u \mathcal{U}_u u_R^I,\ e_R \equiv V_e \mathcal{U}_e e_R^I,\ v_R \equiv V_v \mathcal{U}_v v_R^I \tag{2.54}$$

Since neutral-current interactions will always be symmetrical, it follows that $\bar{f}_R^I \gamma^\mu f_R^I = \bar{f}_R \gamma^\mu f_R$ and $\bar{f}_L^I \gamma^\mu f_L^I = \bar{f}_L \gamma^\mu f_L$, meaning no neutral currents that change flavour exist at the tree level. The administrators engaged the charged present interaction phrases do not always diagonal in terms of mass eigenfields. To illustration,

$$\bar{u}_L^I \gamma^\mu d_L^I = \bar{u}_L \gamma^\mu V_u V_d^\dagger d_L = \bar{u}_L \gamma^\mu V d_L. \tag{2.55}$$

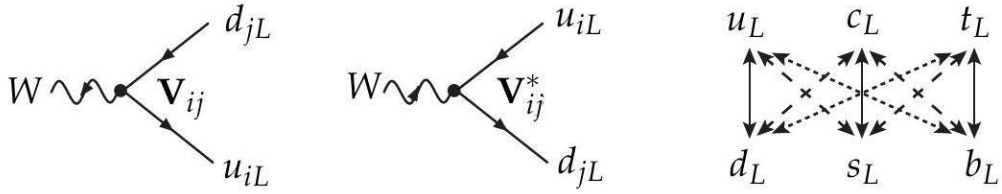

Figure 2.6. Weak charged currents alter the family of quarks (J.I.Illana and A.Jimenez Cano, 2022).

The Cabibbo-Kobayashi-Maskawa (CKM) mixing matrix is represented through the unitary matrix $V \equiv V_u V_d^\dagger$ (M. Kobayashi and T. Maskawa, 1973) which accounts for quark flavour misalignment and induces inter-family transitions ,

$$\mathcal{L}_{CC} = \frac{g}{\sqrt{2}} \sum_{ij} \bar{u}_{Li} \gamma^\mu V_{ij} d_{Lj} W_\mu^\dagger + \text{h.c.}$$

$$= \frac{g}{2\sqrt{2}} \sum_{ij} \bar{u}_i \gamma^\mu (1 - \gamma_5) V_{ij} d_j W_\mu^\dagger + \text{h.c.} \tag{2.56}$$

The FCNC will appear at the level within the loop due to these flavour changes in charged currents, but they will be suppressed (S. L. Glashow,1970).

Assume that, d_j or u_i has degenerate masses, field redefinitions could be used to choose $V_d = V_u$, and quark families would not mix. The matrix elements V_d and V_u are not observable. However, the masses and mixtures are visible. Using the same logic, there is no lepton mixing in a lepton sector with massless neutrinos.

At this point, the number of mixing parameters physically introduced must be discussed. For a general n × n unitary matrix, such as the CKM, the total amount of real parameters is

$$n^2 = n(n-1)/2 \text{ moduli } + n(n+1)/2 \text{ phases.} \tag{2.57}$$

The fact that a few stages can be absorbed by field phase-redefinitions, however, renders them unphysical,

$$u_i \to e^{i\alpha_i} u_i,\ d_j \to e^{i\beta_j} d_j \Rightarrow V_{ij} \to V_{ij} e^{-i(\alpha_i - \beta_j)} \tag{2.58}$$

Consequently, a variety of physical variables is expressed in Eq. (2.59), after $2n-1$ phases are removed.

$$(n-1)^2 = n(n-1)/2 \text{ moduli } + (n-1)(n-2)/2 \text{ phases.} \tag{2.59}$$

Particularly, It is just one parameter (the Cabibbo angle θ_C) for the case of $n = 2$ generations, as follows:

$$V = \begin{pmatrix} \cos\theta_C & \sin\theta_C \\ -\sin\theta_C & \cos\theta_C \end{pmatrix}. \tag{2.60}$$

There are three angles, as well as one phase in the actual case of $n = 3$ generations. In the standard parametrization ,

$$V = \begin{pmatrix} V_{ud} & V_{us} & V_{ub} \\ V_{cd} & V_{cs} & V_{cb} \\ V_{td} & V_{ts} & V_{tb} \end{pmatrix} = \begin{pmatrix} 1 & 0 & 0 \\ 0 & c_{23} & s_{23} \\ 0 & -s_{23} & c_{23} \end{pmatrix} \begin{pmatrix} c_{13} & 0 & s_{13}e^{-i\delta} \\ 0 & 1 & 0 \\ -s_{13}e^{i\delta} & 0 & c_{13} \end{pmatrix} \begin{pmatrix} c_{12} & s_{12} & 0 \\ -s_{12} & c_{12} & 0 \\ 0 & 0 & 1 \end{pmatrix}$$

$$= \begin{pmatrix} c_{12}c_{13} & s_{12}c_{13} & s_{13}e^{-i\delta} \\ -s_{12}c_{23} - c_{12}s_{23}s_{13}e^{i\delta} & c_{12}c_{23} - s_{12}s_{23}s_{13}e^{i\delta} & s_{23}c_{13} \\ s_{12}s_{23} - c_{12}c_{23}s_{13}e^{i\delta} & -c_{12}s_{23} - s_{12}c_{23}s_{13}e^{i\delta} & c_{23}c_{13} \end{pmatrix} \quad (2.61)$$

with $0 \leq \delta \leq 2\pi$ and $c_{ij} \equiv \cos\theta_{ij} \geq 0, s_{ij} \equiv \sin\theta_{ij} \geq 0 (i < j = 1,2,3)$.

The complicated phases is just one cause of CP violation in the SM Lagrangian. The theory of quarks includes three distinct generations at least. Considering that quarks are bound within hadrons by the strong interaction, the values of the CKM parameters are derived from a wide range of hadronic weak decays.(P. A. Zyla et al, 2020).

$$\theta_{12} \equiv \theta_C \approx 13^\circ,\ \theta_{23} \approx 2.3^\circ,\ \theta_{13} \approx 0.2^\circ,\ \delta \approx 68^\circ. \quad (2.62)$$

Surprisingly, every observable that violates the CP condition needs to be proportional to the Jarlskog constant(C. Jarlskog, 1985),which is given by the phase-convention independent, $\mathrm{Im}\left(V_{ij}V_{kl}V_{il}^{*}V_{kj}^{*}\right) = J\sum_{m,n}\epsilon_{ikm}\epsilon_{jln}$. In the standard parametrization $J = c_{12}c_{23}c_{13}^{2}s_{12}s_{23}s_{13}\sin\delta$. The fact that the observed value of $J \approx 3 \times 10^{-5}$ is far lower than its theoretically predicted maximum of $1/(6\sqrt{3}) \approx 0.1$ demonstrates that CP violation is effectively mitigated in the quark area.

Like previously stated, there would be no lepton mixing if neutrinos were massless. However, For neutrino oscillation to occur, neutrinos must mix and have non-degenerate masses, despite their small values. Adding gauge-singlet right handed neutrinos to the standard model with only Yukawa couplings to the Higgs and the lepton doublet is one conceivable minimal expansion of the original SM as suggested in Eqs (2.47) and (2.49). This vSM (R. N. Mohapatra and P. B. Pal, ,1998) is not very satisfying since minuscule Yukawa couplings $_\lambda_v = \sqrt{2}m_v/v \lesssim 10^{-12}$are required to

obtain neutrino masses $m_\nu \lesssim 0.1eV$; this is not only strange but also predicts phenomenology that cannot be tested. Another possibility is that neutrinos are their own antiparticle, a type of fermion known as a Majorana in contrast to the other fermions.

Neutrinos can get gauge invariant Majorana mass components, along with the normal Dirac mass components from Yukawa interactions with the Higgs doublet, allowing for novel pathways for the formation of masses and mixings. Introducing gauge right handed new singlets with a massive Majorana mass terms $m_R \gtrsim 10^{14}GeV$ and Dirac masses $m_D \sim \frac{v}{\sqrt{2}} \sim 100GeV$, the type-I seesaw mechanism (M. Gell-Mann, P. Ramond, and R. Slansky, 1979),(T. Yanagida, 1979) explains the low mass of active neutrinos.

The resulting mass eigenstates include light Majorana neutrinos with masses $m_\nu \approx m_D^2/m_R$ that are very close to $\nu = \nu_L + \nu_L^c$, and super heavy neutrinos with masses $m_N \approx m_R$ and low light-heavy mixings of request m $m_D/m_R \sim \sqrt{m_\nu/m_N}$. Because majorana fields are self-conjugate ($\nu = \nu^c$), their chiral components are connected.

Because of this, the intergenerational lepton mixings now contain additional CP phases that are unable to be absorbed due to the fact that neutrino field phase-redefinitions can no longer take place. In any event, global fits to neutrino oscillations are compatible with three generations of active neutrino flavours $\nu_{\alpha L}(\alpha = e, \mu, \tau)$ that consist of a mixture of the masses of three different types of light neutrino $\nu_{iL}(i = 1,2,3)$

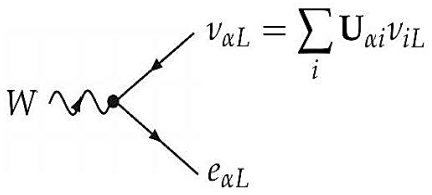

Figure 2.7. Detection of neutrino eigenstate ν_α, and charged lepton e_α(J.I.Illana and A.Jimenez Cano, 2022).

$$v_{\alpha L} = \sum_i U_{\alpha i} v_{iL} \tag{2.63}$$

while $V_v^\dagger$ in is the Pontecorvo-Maki-Nakagawa-Sakata (PMNS) matrix U (B. Pontecorvo, Mesonium and anti-mesonium, 1957), (Z. Maki, 1962). Neutrinos, if they are Majorana particles, then their mass matrix will be diagonalized by a roughly unitary 3x3 block. This block comprises both light and heavy species of neutrinos. The reason for this oscillation occurrence is that the mass disparities between the distinct light mass eigenstates are minimal. enough for the logical overlap v_α , the chance when a (relativistic) neutrino in a flavor quantum state travels (in vacuum) L=t distance and is observed as a flavor in Eqs. (2.64-2.66) and described in Fig.2.8.

$$|v_\alpha; t\rangle = \sum_i U_{\alpha i} e^{-iE_i t} |v_i\rangle,\ E_i \approx E + \frac{m_i^2}{2E} \tag{2.64}$$

$$\Rightarrow \langle v_\beta \mid v_\alpha; t\rangle = \sum_i U_{\beta i}^* U_{\alpha i} e^{-iE_i t} \tag{2.65}$$

$$\Rightarrow\ P(v_\alpha \to v_\beta; L) = \left|\left\langle v_\beta \middle|_\alpha; L\right\rangle\right|^2 = \sum_{ij} U_{\beta i}^* U_{\alpha i} U_{\beta j} U_{\alpha j}^* \exp\left(-i\frac{\Delta m_{ij}^2}{2E}\right) \tag{2.66}$$

That $E \approx p$ is the momentum of the relativistic neutrino with masses m_i and $\Delta m_{ij}^2 \equiv m_i^2 - m_j^2$. The reason why charged lepton flavours don't oscillate is $|\Delta m_{ij}^2| \ll \Delta m_{\mu e}^2$ (B. Pontecorvo, 1967).

The PMNS matrix in the conventional parametrization is as follows:

$$U = \begin{pmatrix} U_{e1} & U_{e2} & U_{e3} \\ U_{\mu 1} & U_{\mu 2} & U_{\mu 3} \\ U_{\tau 1} & U_{\tau 2} & U_{\tau 3} \end{pmatrix}$$

$$= \begin{pmatrix} c_{12}c_{13} & s_{12}c_{13} & s_{13}e^{-i\delta} \\ -s_{12}c_{23} - c_{12}s_{23}s_{13}e^{i\delta} & c_{12}c_{23} - s_{12}s_{23}s_{13}e^{i\delta} & s_{23}c_{13} \\ s_{12}s_{23} - c_{12}c_{23}s_{13}e^{i\delta} & -c_{12}s_{23} - s_{12}c_{23}s_{13}e^{i\delta} & c_{23}c_{13} \end{pmatrix} \begin{pmatrix} 1 & 0 & 0 \\ 0 & e^{\frac{i\alpha_{21}}{2}} & 0 \\ 0 & 0 & e^{\frac{i\alpha_{31}}{2}} \end{pmatrix} \tag{2.67}$$

When neutrinos are Majorana particles, as was indicated above, then additional phases α_{21}, α_{31} are necessary; however, the remaining parameters, despite the fact that their values vary, are comparable to the CKM mixing parameters.

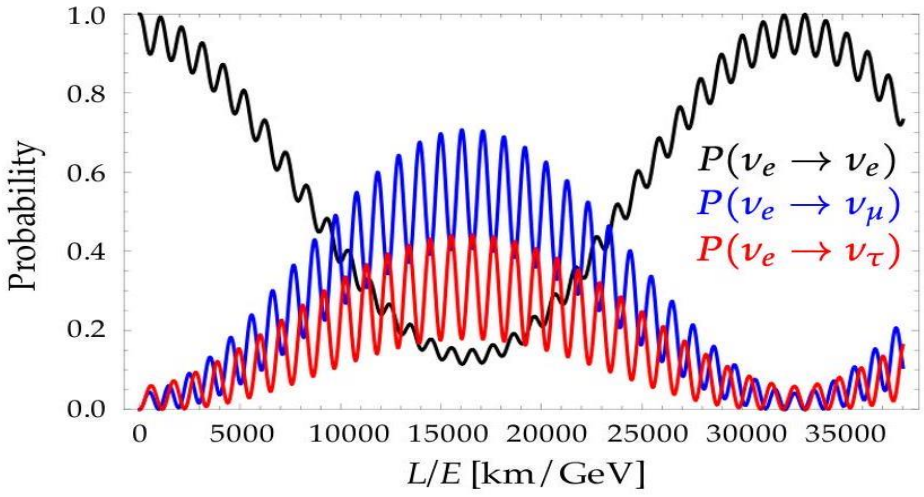

Figure 2.8. Probabilities of a vacuum oscillating at a given v_e from experimental data (J.I.Illana and A.Jimenez Cano, 2022).

Neutrino mass variation and combining variables are compelled by a perfect numeral of ocillation experiments by heliacal, aerial, accelerator and nuclear neutrinos(E. K. Akhmedov, 2007).

$$\Delta m_{21}^2 \approx 7.5 \times 10^{-5} eV^2,\ |\Delta m_{31}^2| \approx 2.5 \times 10^{-3} eV^2 \quad (2.68)$$

$$\theta_{12} \equiv \theta_{\odot} \approx 34°,\ \theta_{23} \equiv \theta_{atm} \approx 49°,\ \theta_{13} \approx 8°. \quad (2.69)$$

The appropriate amount of the Dirac phase δ rely on the Δm_{31}^2. The ordering of neutrino masses is normal (NO) or inverted (IO). A number that conserves CP, such as $\delta \approx 180°$, is favoured by NO, but IO favours a nearly maximal value that violates CP, such as $\delta \approx 280°$. In addition, the oscillations are immune to the influence of Majorana phases. The discovery of neutrinoless double-beta decays will give rise to a certain a kind of experiment it can clarify if neutrinos are of the Dirac or Majorana variety(P. F. de Salas, 2021)

3. THE NEUTRINO MASS: A MASSIVE PROBLEM

The Standard Model's neutrino section can be considered unique for the following reasons: the mixing angles of neutrinos are noticeably bigger than those of quarks, and their masses are at least six orders of magnitude less than those of the other fermions. Attempt, as is only natural, to tie the structures observed in the masses and mixing angles of neutrinos to a more fundamental theory.

3.1. The Seesaw Models I & II& III

3.1.1. The Seesaw Model Type I

It is one of the less complicated ways of including a neutrino mass. It was first presented in 1980 by R. N. Mohapatra and G. Senjanovi'c to give a reason for the modest neutrino masses that are a direct outcome of the heavy right-handed neutrinos. (R. N. Mohapatra and G. Senjanovi'c, 1980). This mass production can be attributed to an imbalance of right-handed and left-handed states.The Lagrangian is

$$\mathcal{L}_{\text{seesaw}} = -\frac{1}{2}\bar{n^c}Mn + \text{ h.c.}$$

with the neutrino fields

$$n = \begin{pmatrix} \nu_L \\ (\nu_R)^c \end{pmatrix}$$

and the mass matrix

$$M = \begin{pmatrix} 0 & m_D \\ m_D & m_M \end{pmatrix}$$

The ν_R, are right handed fermions that are SM singlets.. Because of this, we can consider them to be sterile neutrinos. However, in traditional seesaw models, they

contribute with a significant amount of weight and are irrelevant to oscillation testing. When we make the assumption that m_M is smaller than m_D, we are able to integrating ν_R to get the seesaw formula is written as:

$$m_\nu \simeq \frac{m_D^2}{m_M}$$

It has a mass of order m_M for heavy neutrinos. At angles on the order of m_D/m_M, the light and heavy neutrino states mix.

The concept readily extends to encompass three generations of left handed neutrinos. The mass matrix is:

$$\mathrm{M} = \begin{pmatrix} 0 & m_\mathrm{D} \\ m_\mathrm{D}^\mathrm{T} & m_\mathrm{M} \end{pmatrix}$$

The diagonalization of M can be obtained via the unitary matrix U:

$$\mathrm{M_{diag}} = \begin{pmatrix} \mathrm{m_\nu} & 0 \\ & \mathrm{m_N} \end{pmatrix} = \mathrm{UMU^T}$$

Approximately we have

$$\mathrm{U} \simeq \begin{pmatrix} 1 & -\mathrm{m_D m_M^{-1}} \\ \mathrm{m_D m_M^{-1}} & 1 \end{pmatrix}$$

The matrix of the effective light neutrino masses can be expressed as a seesaw formula.

$$\mathrm{m_\nu} \simeq -\mathrm{m_D m_M^{-1} m_D^T}$$

3.1.2. The Seesaw Model Type II

In this type, there are no heavy right handed sterilized neutrinos. Instead, a second Higgs field, known as a triplet under SU(2)L, is added to the Standard Model and with Y = 2. The Higgs boson and SU (2) L doublet via Y = −1.

$$\mathcal{L}_{\text{type II}} \supset y_{\alpha\beta}\bar{L^{c}_{\alpha}}\Delta L_{\beta} + \mu_{\Delta}\widetilde{H}^{\dagger}\Delta H.$$

Other couplings in the Higgs sector exist, but they are not relevant here. Applying the definition $\widetilde{H} = i\sigma^{2}H^{*}$, the process involves interchanging the top and lower components of the Higgs doublet, guarantees that the new item will continue to change in the doublet form of the SU(2)L group. These pairings are permitted by symmetry because a singlet can be formed by joining two SU(2) doublets and one SU(2) triplet. Remember that the "spins" of fundamental particles are described by SU(2) representations. It is the weak isospin, not the real spin, that the SU(2)L is referring to here. A doublet represents an isospin 1/2 state, while a triplet represents a 1 state. Like genuine spins, isospins can be introduced. Using the same requirements, a combination of two isospin 1/2 states, one isospin 1, and one isospin 0 state yields an SU(2) singlet.

$$H = \begin{pmatrix} H^{+} \\ H^{0} \end{pmatrix} \qquad L\alpha = \begin{pmatrix} V_{L,\alpha} \\ e_{L,\alpha} \end{pmatrix}$$

$$\Delta = \begin{pmatrix} \delta^{+}/\sqrt{2} & \delta^{++} \\ \delta^{0} & -\delta^{+}/\sqrt{2} \end{pmatrix}$$

According to SU(2) conversion $U = e^{i\alpha a\sigma a/2}$. Those states evolve as $H \rightarrow UH$, $L\alpha \rightarrow UL\alpha$ and $\Delta \rightarrow U\Delta U U^{\dagger}$. When$H^{0}$ obtains a vacuum expectation value, the following type of mass is obtained

$$\mathcal{L}_{\text{mass type II}} \sim y_{\alpha\beta\mu\Delta}\ \frac{v^{2}}{M_{\Delta}^{2}}\ \overline{v^{c}_{L\alpha}}\ \ v_{LB}$$

3.1.3. The Seesaw Model Type III

In this type, SU(2) triplets $\Sigma_{R,\beta}$ are introduced to replace the type I seesaw right handed singlet neutrinos. The pertinent connections include

$$\mathcal{L}_{\text{type III}} \supset Y_{\Sigma,\alpha\beta} H \bar{L}^{c}_{\alpha} \Sigma_{R,\beta} + \frac{1}{2} M_{\Sigma,\alpha\beta} \bar{\Sigma}^{c}_{R,\alpha} \Sigma_{R,\beta},$$

The neutrino mass term that arises as a consequence is given as

$$\mathcal{L}_{\text{mass , type III}} \sim v^2 \left(y_{\Sigma}^{T} M_{\Sigma}^{-1} y_{\Sigma}\right)_{\alpha\beta} \bar{\nu}^{C}_{L\alpha} \nu_{L\beta}.$$

The 3 basic seesaw models

Right-handed singlet: (seesaw I)	**scalar triplet: (seesaw II)**	**firmion triplet (seesaw III)**
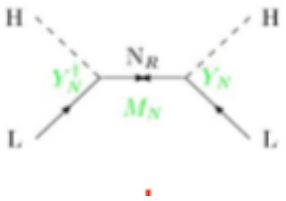	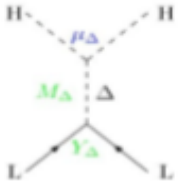	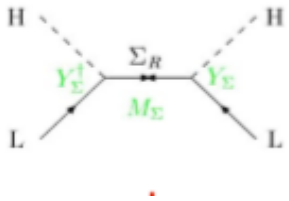
$m_\nu = Y_N^T \frac{1}{M_N} Y_N v^2$	$m_\nu = Y_\Delta \frac{\mu_\Delta}{M_\Delta^2} v^2$	$m_\nu = Y_\Sigma^T \frac{1}{M_\Sigma} Y_\Sigma v^2$

Figure 3.1. three typys seesaw models (T. Hambye, 2009)

3.2. Radiative Neutrino Mass Models

It is particularly interesting to provide an explanation for why the mass of neutrinos is so unbelievably tiny in comparison to the masses of the many several fermions found in the SM, and the radiative models are particularly appealing for this purpose. Furthermore, masses may originate from a number of different sources, each of which may have a preexisting hierarchy of mass distributions of their own.

It is believed, in accordance with the Glashow-Weinberg-Salam theory of electroweak interactions, that all fermions (with the exception of neutrinos) the acquisition of mass occurs through the interaction of particles with the Higgs boson via Yukawa couplings.. This is in contrast to the idea that neutrinos acquire mass through electroweak interactions. This happens once the symmetry in the system spontaneously breaks down. The zero order mass, on the other hand, does not exist in a radiative model since the presence of this term is prohibited by some symmetry. In its place, mass is generated at a higher orders during the perturbative expansion, which takes place at the loop level. This occurs due to the fact that the radiative model possesses some symmetry.

3.2.1. Zee-Wolfenstein Model

The model is known as being among the most popular radiative models (A. Zee, 1980). It adds two extra scalars to the SM's scalar sector: one charged singlet., χ+ and one doublet $\phi_2 = \begin{pmatrix} \phi_2^+ \\ \phi_2' \end{pmatrix}$. Additionally, it is expected that leptons and ϕ_2 do not couple. Tree level neutrino masses derived from a renormalizable Lagrangian are not achievable in this model, although one loop level neutrino masses are. A one-loop procedure like this is depicted in Fig 3.2. The intriguing aspect of this model is that it proposes a unique configuration for the neutrino mass matrix:

$$\mathcal{M}_\nu = \begin{pmatrix} 0 & f_{\mu e}(m_\mu^2 - m_e^2) & f_{\tau e}(m_\tau^2 - m_e^2) \\ f_{\mu e}(m_\mu^2 - m_e^2) & 0 & f_{\tau\mu}(m_\tau^2 - m_\mu^2) \\ f_{\tau e}(m_\tau^2 - m_e^2) & f_{\tau\mu}(m_\tau^2 - m_\mu^2) & 0 \end{pmatrix}$$

Sadly, despite lengthy study, the Zee-Wolfenstein hypothesis has been disproven by experiments. (X. G. He, 2004)

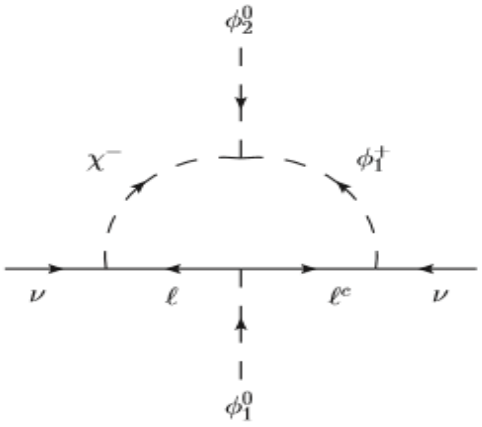

Figure 3.2. Zee-Wolfenstein neutrino mass generation by one-loop (Bouchand, 2012).

3.2.2. Zee-Babu Model

The right-handed neutrinos are excluded from this set up. In this model, which was introduced between 1985 and 1987 (K. S. Babu, 1988),(F. R. Klinkhamer and N. S. Manton, 1984), (V. Kuzmin, V. Rubakov and M. Shaposhnikov, 1985), (R. N. Mohapatra and G. Senjanovi´c, 1980) and (G. B. Gelmini and M. Roncadelli,1981). In this model, the Standard Model is expanded to include two charged singlet Higgs fields: a singly charged $\chi+$ and a doubly charged $\zeta++$. Due to the use of two-loop diagrams, the resulting neutrino masses are finite and naturally tiny Fig. 3.3. The model's major prediction is one of the neutrinos that has no mass. However, this suggests that certain leptons will undergo lepton number violating decays such $\mu \rightarrow$ eee and $\tau \rightarrow \mu\mu\mu$ and will

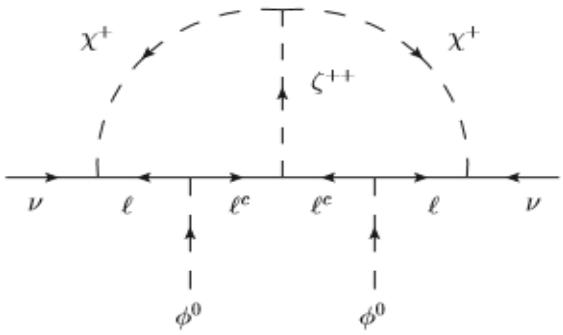

Figure 3.3. Neutrino mass by Two-loop (Bouchand, 2012).

3.2.3. Two-W Mechanism

One neutrino singlet N is the bare minimum model need to provide mass for the neutrinos. Each of the flavour eigenstates only have one linear mixing that receives a tree-level Majorana mass value and the other two flavours appearing to remain massless. These zeros aren't symmetrically shielded, though, and nothing mandates that they stay that way after radiative corrections.

The other neutrinos are actually generated by a two-loop correction, Fig. 3.4. Although not entirely a radiative model , this model from (K. S. Babu and E. Ma, 1988) ,was formally intriguing because it suggested that the W-boson, which had only been found five years previously, may only affect the creation of neutrino mass at higher orders. Yet, the relevant neutrinos' masses from this two-loop, doubly GIM suppressed mechanism are utterly insignificant.

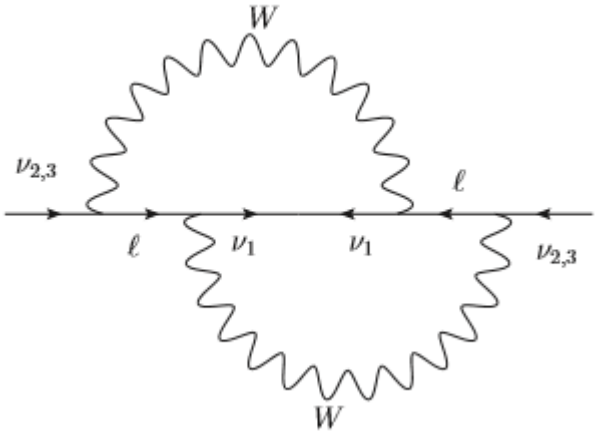

Figure 3.4. The mass generation of two W-Mechanism (Bouchand, 2012).

4. THE SCOTOGENIC MODEL

Significant guideposts since efforts to lay out the concept of new physics beyond the SM are the recent observation of a Higgs boson with a mass around 126GeV at the Large Hadron Collider (LHC) (G. Aad et al. 2012) and the assurance of the neutrino blending boundary $\sin\theta_{13}$ at neutrino-wavering tests (F.P. An et al., 2012).

Other factor that any realistic scenario for new physics is the need to describe the quarter of the cosmic energy budget assumed to be related to dark matter (Beringer et al. 2012, P.A.R. Ade et al.2012). The scotogenic model (E. Ma, 2006) proposes that neutrinos acquire mass radially via one-loop level Feynman diagram with nonstandard particles consisting of scalars and fermions, one of which functions as dark matter (DM) run in the loop. In this framework (S.Y. Ho and Tandean, 2013), a few of the effects of the preceding trial findings, namely the decays of the Higgs boson h into final states containing the new particles, with the lightest of these particles expected to be fermionic cold DM. They found that unusual decays of h might have rates that were previously probed by existing LHC data, and that the scotogenic effects on $h \rightarrow \gamma\gamma$, γZ would be testable in forthcoming measurements. This was determined after taking into account a number of experimental and theoretical restrictions.

Additional tests on this model using e^+e^-colliders were motivated in part by the availability of a sizable amount of historical data from LEPII (A. Heister et al. 2004), (D. Buskulic et al. 1996) that may be relevant to the model parameter space of interest and in part by the growing likelihood that the International Linear Collider (ILC) will be realized in the near future.

4.1. Interactions and Yukawa Couplings

A scalar doublet, η, and three singlet Majorana fermions, $N_{1,2,3}$, that are all odd under a strictly preserved Z_2 symmetry are the only particle content beyond the SM one in

the simplest form of the scotogenic model (E. Ma, 2006). All of the SM particles are Z_2 even. The new particle with the least mass among the nonstandard particles must therefore be stable and able to function as DM candidate. In the previous studies that particle is assumed to be N_1.

The Lagrangian responsible for the connections between the scalar particles and the gauge bosons in this model is given as

$$\mathcal{L} = (\mathcal{D}^{\rho}\Phi)^{\dagger}\mathcal{D}_{\rho}\Phi + (\mathcal{D}^{\rho}\eta)^{\dagger}\mathcal{D}_{\rho}\eta - \mathcal{V}$$

where $\mathcal{D}_{\rho}$ is the familiar covariant derivative constructed using the SM gauge fields, and the potential $\mathcal{V}$ is (E. Ma, 2006)

$$\mathcal{V} = \mu_1^2\Phi^{\dagger}\Phi + \mu_2^2\eta^{\dagger}\eta + \frac{1}{2}\lambda_1(\Phi^{\dagger}\Phi)^2 + \frac{1}{2}\lambda_2(\eta^{\dagger}\eta)^2$$
$$+\lambda_3(\Phi^{\dagger}\Phi)(\eta^{\dagger}\eta) + \lambda_4(\Phi^{\dagger}\eta)(\eta^{\dagger}\Phi) + \frac{1}{2}\lambda_5[(\Phi^{\dagger}\eta)^2 + (\eta^{\dagger}\Phi)^2]$$

in accordance with electroweak symmetry breaking we have

$$\Phi = \begin{pmatrix} 0 \\ \frac{1}{\sqrt{2}}(h+v) \end{pmatrix}, \qquad \eta = \begin{pmatrix} H^{+} \\ \frac{1}{\sqrt{2}}(\mathcal{S} + i\mathcal{P}) \end{pmatrix}$$

With v is the vacuum expectation value (VEV) and h is physical Higgs boson. The VEV of η must be zero according to the Z_2 symmetry. Then, the masses of S, P, and $H^{\pm}$ are provided as.

$$m_{\mathcal{S}}^2 = m_{\mathcal{P}}^2 + \lambda_5 v^2 = \mu_2^2 + \frac{1}{2}(\lambda_3 + \lambda_4 + \lambda_5)v^2, \qquad m_H^2 = \mu_2^2 + \frac{1}{2}\lambda_3 v^2.$$

Consider the λ_5 is very small (Kubo, 2006), $|\lambda_5| \ll |\lambda_3 + \lambda_4|$, the suggestion $m_{\mathcal{S},\mathcal{P}}$ are almost sterile, $\left|m_{\mathcal{S}}^2 - m_{\mathcal{P}}^2\right| = |\lambda_5| v^2 \ll m_{\mathcal{S}}^2 \simeq m_{\mathcal{P}}^2$. In L, the interactions of the η to h, the photon A, and the Z boson are given by

$$\begin{aligned}\mathcal{L} \supset\ & [(\mu_2^2 - m_{\mathcal{S}}^2)\mathcal{S}^2 + (\mu_2^2 - m_{\mathcal{P}}^2)\mathcal{P}^2 + 2(\mu_2^2 - m_H^2)H^+H^-]\frac{h}{v} \\ & + ie(H^+\partial^\rho H^- - H^-\partial^\rho H^+)A_\rho + e^2 H^+H^-A^2 + \frac{eg}{c_w}(1 - 2s_w^2)H^+H^-A^\rho Z_\rho \\ & + \frac{g}{2c_w}[\mathcal{P}\,\partial^\rho \mathcal{S} - \mathcal{S}\,\partial^\rho \mathcal{P} + i(1 - 2s_w^2)(H^+\partial^\rho H^- - H^-\partial^\rho H^+)]Z_\rho,\end{aligned}$$

The Lagrangian giving the interactions of N_k is

$$\mathcal{L}_N = -\frac{1}{2} M_k \bar{N}_k^c P_R N_k + \mathcal{Y}_{rk}\left[\bar{\ell}_r H^- - \frac{1}{\sqrt{2}}\bar{\nu}_r(\mathcal{S} - i\mathcal{P})\right] P_R N_k + \text{H.c.},$$

M_k denote to masses, summation over k,r = 1,2,3 is implicit, and c denote to charge conjugation, $P_R = \frac{1}{2}(1 + \gamma_5)$, and $\ell_{1,2,3} = e, \mu, \tau$. The Yukawa couplings of N_k comprise the matrix

$$\mathcal{Y} = \begin{pmatrix} Y_{e1} & Y_{e2} & Y_{e3} \\ Y_{\mu 1} & Y_{\mu 2} & Y_{\mu 3} \\ Y_{\tau 1} & Y_{\tau 2} & Y_{\tau 3} \end{pmatrix}$$

Where $Y_{\ell_r k} = \mathcal{Y}_{rk}$.

The intrinsic S, P, and N_k of one-loop diagrams allow the light neutrinos to radiatively gain masses. The mass eigenvalues m_j are given by

$$\text{diag}(m_1, m_2, m_3) = \mathcal{U}^\dagger \mathcal{M}_\nu \mathcal{U}^*$$

$$\Lambda_k = \frac{\lambda_5 v^2}{16\pi^2 M_k}\left[\frac{M_k^2}{m_0^2 - M_k^2} + \frac{2M_k^4 \ln(M_k/m_0)}{(m_0^2 - M_k^2)^2}\right], \qquad m_0^2 = \frac{1}{2}(m_{\mathcal{S}}^2 + m_{\mathcal{P}}^2),$$

where U is the Pontecorvo-Maki-Nakagawa-Sakata (PMNS)(B. Pontecorvo, 1968) unitary matrix. In the equation for Λ_k relates we have $m_0 \simeq m_S \simeq m_P$. For the U matrix, we select the PDG parametrization (Beringer et al. 2012)

$$\mathcal{U} = \tilde{u}\mathrm{diag}\left(e^{i\alpha_1/2}, e^{i\alpha_2/2}, 1\right)$$

$$\tilde{u} = \begin{pmatrix} c_{12}c_{13} & s_{12}c_{13} & s_{13}e^{-i\delta} \\ -s_{12}c_{23} - c_{12}s_{23}s_{13}e^{i\delta} & c_{12}c_{23} - s_{12}s_{23}s_{13}e^{i\delta} & s_{23}c_{13} \\ s_{12}s_{23} - c_{12}c_{23}s_{13}e^{i\delta} & -c_{12}s_{23} - s_{12}c_{23}s_{13}e^{i\delta} & c_{23}c_{13} \end{pmatrix},$$

where $\delta \in [0,2\pi]$ and $\alpha 1,2 \in [0,2\pi]$, $c_{mn=}\cos\theta_{mn} \geq 0$, and $s_{mn} = \sin\theta_{mn} \geq 0$. A new inspection of information pertaining to the global neutrino oscillation reveals (M.C. Gonzalez-Garcia, 2012)

$$s_{12}^2 = 0.302^{+0.013}_{-0.012}, \qquad s_{23}^2 = 0.413^{+0.037}_{-0.025}, \qquad s_{13}^2 = 0.0227^{+0.0023}_{-0.0024}, \delta = (300^{+66}_{-138})^\circ$$

We choose Y_{ek} and $Y_{\mu k}$ in terms of $Y_k \equiv Y_{\tau k}$ (S. Y. Ho and Tandean, 2014) and the others are given as

$$Y_{e1} = \frac{-c_{12}c_{13}Y_1}{c_{12}c_{23}s_{13}e^{i\delta} - s_{12}s_{23}}, \qquad Y_{\mu 1} = \frac{c_{12}s_{23}s_{13}e^{i\delta} + s_{12}c_{23}}{c_{12}c_{23}s_{13}e^{i\delta} - s_{12}s_{23}} Y_1$$

$$Y_{e2} = \frac{-s_{12}c_{13}Y_2}{s_{12}c_{23}s_{13}e^{i\delta} + c_{12}s_{23}}, \qquad Y_{\mu 2} = \frac{s_{12}s_{23}s_{13}e^{i\delta} - c_{12}c_{23}}{s_{12}c_{23}s_{13}e^{i\delta} + c_{12}s_{23}} Y_2$$

$$Y_{e3} = \frac{s_{13}Y_3}{c_{23}c_{13}e^{i\delta}}, \qquad Y_{\mu 3} = \frac{s_{23}Y_3}{c_{23}}$$

That are equivalent to the mass eigenvalues.

$$m_1 = \frac{\Lambda_1 Y_{e1}^2 e^{-i\alpha_1}}{c_{12}^2 c_{13}^2}, \qquad m_2 = \frac{\Lambda_2 Y_{e2}^2 e^{-i\alpha_2}}{s_{12}^2 c_{13}^2}, \qquad m_3 = \frac{\Lambda_3 Y_3^2}{c_{13}^2 c_{23}^2}.$$

Where $m_{1,2,3}$be real and nonnegative this means

$$\alpha_1 = \arg(\Lambda_1 Y_{e1}^2), \qquad \alpha_2 = \arg(\Lambda_2 Y_{e2}^2), \qquad \arg(\Lambda_3 Y_3^2) = 0$$

4.2. Solutions for Yukawa couplings y_{rk}

Three Yukawa coupling pairs and the relationships between them ($Y_{ek}\ Y_{\mu k}$) with k = 1, 2, 3 can be properly defined in the form of of $Y_k = Y_{\tau k}$. There are a total of 27 Collections of possible solutions. Each set's pairs can be written as ($Y_{ek}\ Y_{\mu k}$) = ez, zYk, where z i= a, b, or c and (see references in (S. Y. Ho and Tandean, 2014))

$$\bar{e}_a = \frac{-c_{12}c_{13}}{c_{12}c_{23}s_{13}e^{i\delta} - s_{12}s_{23}}, \qquad \bar{\mu}_a = \frac{c_{12}s_{23}s_{13}e^{i\delta} + s_{12}c_{23}}{c_{12}c_{23}s_{13}e^{i\delta} - s_{12}s_{23}}$$

$$\bar{e}_b = \frac{-s_{12}c_{13}}{s_{12}c_{23}s_{13}e^{i\delta} + c_{12}s_{23}}, \qquad \bar{\mu}_b = \frac{s_{12}s_{23}s_{13}e^{i\delta} - c_{12}c_{23}}{s_{12}c_{23}s_{13}e^{i\delta} + c_{12}s_{23}}$$

$$\bar{e}_c = \frac{s_{13}e^{-i\delta}}{c_{23}c_{13}}, \qquad \bar{\mu}_c = \frac{s_{23}}{c_{23}}$$

with. $c_{mn=}\cos\theta_{mn}$, $s_{mn} = \sin\theta_{mn}$

We see that not all solutions result in at least two non-zero masses among the $m_{1,2,3}$ eigenvalues reported in certain other radioneutrino mass models(C. Boehm, 2008),(A. Ahriche and S. Nasri, 2013),(G. Guo, X.G. He, 2012) , leading to the possibility of $Y_{\ell k}$ solutions with the $\Lambda_{1,2,3}$ model's specifics concealed.

4.3. Dark Matter

In a result of Z_2 symmetry where in only nonstandard model particles are odd under this symmetry, the lightest odd particle has stability and so it is classified as dark matter candidate. In this inquiry, we take a look at a scenario in which the lightest

Majorana singlet fermion, N_1 is the dark matter particle and it is degenerate in mass with N_2. The most important contributions to the annihilation cross-section σ_{ann} produce using the tree-level processes $N_1\bar{N}_1 \to \ell_i^- \ell_j^+$ and $N_1\bar{N}_1 \to v_i\bar{v}_j$νi intervened by the interchange of $H^{\pm}$and (S,P), respectively and upon replacing N_1 by N_2. The acquired annihilation through area can be widened in regards of the relative speed v_{rel} of the $N_{1,2}\overline{N}_{1,2}$ pair in their center-of-mass frame as $\sigma_{ann}\, v_{rel} = a + bv_{rel}^2 + \mathcal{O}(v_{rel}^4)$. The relic density Ω can be written in

$$\Omega\hat{h}^2 = \frac{1.07 \times 10^9 x_f \mathrm{GeV}^{-1}}{\sqrt{g_*} m_{\mathrm{Pl}}\left[a + 3(b - a/4)/x_f\right]},$$
$$x_f = \ln \frac{0.0764 c(2+c)\left(a + 6b/x_f\right) M_1 m_{\mathrm{Pl}}}{\sqrt{\delta_* x_f}},$$

where $c \simeq 1/2, m_{\mathrm{Pl}} = 1.22 \times 10^{19}\mathrm{GeV}$ is the Planck mass, g∗ is the number of relativistic degrees of freedom below the freezeout temperature $T_f = M_1/x_f$, and $\hat{h}$ denotes the Hubble parameter. The statements of a and b can be seen in (S. Y. Ho and J. Tandean,In, 2013) and also in (T. Kitabayashi, 2022). It was mentioned that when the DM and the new scalar particle are degenerate in mass, their coannihilation methods is essential to the DM relic density. Consequently, in order to compensate for DM relic density, the dark matter particle has to be heavier which in turn yields more small BR(μ → eγ) accordingly strong constraints (T. Kitabayashi, 2021). Consequently, to get beyond the strict limitations on the parameter space, We select $M_1 < m_0$ to rule out the potential of the coannihilation of new scalar particles and DM. We consider the situation where the lightest and following to lightest singlet fermionsN_1 and N_2 are degenerate in masses and assume the part of the DM. We mention to (D. Suematsu, 2010) and (G. Faisel, 2014) for further talks and information regarding this case.

4.4. Constraints.

The neutrino masses are assumed to follow the standard order of (m1 < m2 < m3). Several of the neutrino parameters have values that can be determined with sufficient precision using a variety of experiments. We incorporate the findings of the most current fit to the worldwide neutrino oscillations data into our study.

Concerning the cosmic constraints on the sum of neutrino masses, the tightest 2σ bound using CMB temperature, polarization, and lensing measurements from the Planck spacecraft, Observations by BAO H(z) information, and Supernovae Ia data constraint $\sum m_i < 0.12\text{eV}$. Neutrino less double beta decay experiments can set constraint on the quantity $\langle m \rangle_{ee}$defined as $\langle \mathrm{m} \rangle_{\mathrm{ee}} = \mathrm{m}_1 \mathrm{U}_{\mathrm{e1}}^2 + \mathrm{m}_2 \mathrm{U}_{\mathrm{e2}}^2 + \mathrm{m}_3 \mathrm{U}_{\mathrm{e3}}^2$. The upper limit reads $|\langle m \rangle_{ee}| < 0.06 - 0.2\text{eVe}$ at the 95% confidence level. We require the relevant parameter space to satisfy the bound $|\langle m \rangle_{ee}| < 0.06$ eV. Furthermore, we need to use the outcomes of latest adjustments to neutrino oscillations data.

$$32.0 < \frac{|\Delta m_{31}^2|}{\Delta m_{21}^2} < 36.0$$

According to the 90%CL confidence intervals for the data on $\Delta \mathrm{m}_{31}^2$and $\Delta \mathrm{m}_{21}^2$. The Yukawa interactions can lead to lepton flavor violation (LFV) processes(T. Toma and A. Vicente, 2014).The existing experimental limits on an important class of LFV processes are $\mathrm{BR}(\mu \to e\gamma) < 4.2 \times 10^{-13}$ (A. M. Baldini et al. 2016), $\mathrm{BR}(\tau \to e\gamma) < 3.3 \times 10^{-8}$ (B. Aubert et al. 2010),and $\mathrm{BR}(\tau \to \mu\gamma) < 4.4 \times 10^{-8}$ (B. Aubert et al. 2010). The branching ratios corresponding to the processes are given as (T. Toma and A. Vicente, 2014)

$$\mathrm{BR}\left(\ell_\alpha \to \ell_\beta \gamma\right) = \frac{3(4\pi^3)\alpha}{4G_F^2} |A_D|^2 \mathrm{BR}\left(\ell_\alpha \to \ell_\beta v_\alpha \bar{v}_\beta\right)$$

Where

$A_D = \sum_{i=1}^{3} \frac{y_{i\beta}^* y_{i\alpha}}{2(4\pi)^2 M_{H^\pm}^2} \mathcal{F}(\xi_i)$

with $\xi_i = M_i^2 / M_{H^+}^2$, and F(x) can be expressed as

$$\mathcal{F}(x) = \frac{1 - 6x + 3x^2 + 2x^3 - 6x^2 \log x}{6(1-x)^4}$$

The flavor-diagonal analogue of the earlier FLV processes causes a change in the anomalous magnetic moment of the lepton ℓi , which may be expressed as (E. Ma and M. Raidal, 2001)

$$\Delta a_{\ell_i} = \frac{-m_{\ell_i}^2}{16\pi^2 m_H^2} \sum_k |y_{ik}|^2 \mathcal{F}(M_k^2 / m_H^2)$$

Among these, the anomalous magnetic moment a_μ can lead to a stringent bounds on the scotogenic parameter space. Currently, the discrepancy between SM predictions and actual values of a_μ is given by $a_u^{exp} - a_u^{SM} = (2.51 \pm 0.59) \times 10^{-9}$.

For the DM candidate N_1, the cross section part, which is unaffected by spin resulting by the Higgs interaction can be written as, the interactions with nucleons manifest at the one-loop level. (J. Liu, et al. 2022).

$$\sigma_{SI} = \frac{4}{\pi} \frac{M_1^2 m_p^2}{(M_1 + m_p)^2} m_p^2 \left(\frac{\Lambda_q}{m_q}\right)^2 f_p^2$$

Where m_p is the proton mass, $f_p \approx 0.3$ is the scalar form factor, and the effective scalar coupling $\Lambda_q$is

$$\Lambda_q = -\frac{y_1^2}{16\pi^2 M_h^2 M_1}\left[\lambda_3 G_1\left(\frac{M_1^2}{M_{\eta^\pm}^2}\right) + \frac{\lambda_3+\lambda_4}{2} G_1\left(\frac{M_1^2}{M_{R,I}^2}\right)\right] m_q,$$

With

$$G_1(x) = \frac{x + (1-x)\log(1-x)}{x}.$$

The couplings λ_3 , λ_4 = 0.01 to avoid the strong constraints from dark matter direct detection.

4.5. Global fit of Neutrino Oscillation

An improved global fit of neutrino oscillation data is offered, but only within the most fundamental three-neutrino paradigm. Mainly, the most recent analysis of data from the Sudbury Neutrino Observatory and IceCube DeepCore are offered, in addition to the material already considered, addressing the atmospheric and solar sectors.

In addition to the long-baseline T2K and NOvA observations, the most recent electron antineutrino data from the Daya Bay and REN reactor investigations were used in that analysis. Neutrino 2020 is where these results were first presented. Overall, these recent analyses lead to improved readings of θ_{13}, θ_{12}, Δm_{21}^2, and $|\Delta m_{31}^2|$.

Although the atmospheric angleθ_{23} is most closely matched by the second octant, solutions in the first octant are still acceptable up to a value of ~2.4σ. For standard (inverted) neutrino mass ordering, the preferred value of for CP-violation observations. Normal neutrino mass ordering still wins out in the global analysis, but only by a margin of 2.5σ. This inclination is less strong than that discovered in earlier global studies.

Two upper limits on the total neutrino mass are provided by the same cosmic data set, with values of $\Sigma m_\nu < 0.12$ (0.15) eV under the standard (inverted) neutrino mass ordering scenario. Bounds on the neutrino mixing parameters and masses are presented in this recent global fit analysis, which accounts for all of the available neutrino physics inputs. The results are summarized in Table 4.1.

Table 4.1. Description of the parameters for neutrino oscillations defined by the global analysis (D.V.Foreroet al. 2021)

parameter	best fit $\pm$ 1σ	2σ range	3σ range
$\Delta m^2_{21}[10^{-5}\mathrm{eV}^2]$	$7.50^{+0.22}_{-0.20}$	7.12–7.93	6.94–8.14
$\lvert\Delta m^2_{31}\rvert[10^{-3}\mathrm{eV}^2]$ (NO)	$2.55^{+0.02}_{-0.03}$	2.49–2.60	2.47–2.63
$\lvert\Delta m^2_{31}\rvert[10^{-3}\mathrm{eV}^2]$ (IO)	$2.45^{+0.02}_{-0.03}$	2.39–2.50	2.37–2.53
$\sin^2\theta_{12}/10^{-1}$	3.18 ± 0.16	2.86–3.52	2.71–3.69
$\theta_{12}/^\circ$	34.3 ± 1.0	32.3–36.4	31.4–37.4
$\sin^2\theta_{23}/10^{-1}$ (NO)	5.74 ± 0.14	5.41–5.99	4.34–6.10
$\theta_{23}/^\circ$ (NO)	49.26 ± 0.79	47.37–50.71	41.20–51.33
$\sin^2\theta_{23}/10^{-1}$ (IO)	$5.78^{+0.10}_{-0.17}$	5.41–5.98	4.33–6.08
$\theta_{23}/^\circ$ (IO)	$49.46^{+0.60}_{-0.97}$	47.35–50.67	41.16–51.25
$\sin^2\theta_{13}/10^{-2}$ (NO)	$2.200^{+0.069}_{-0.062}$	2.069–2.337	2.000–2.405
$\theta_{13}/^\circ$ (NO)	$8.53^{+0.13}_{-0.12}$	8.27–8.79	8.13–8.92
$\sin^2\theta_{13}/10^{-2}$ (IO)	$2.225^{+0.064}_{-0.070}$	2.086–2.356	2.018–2.424
$\theta_{13}/^\circ$ (IO)	$8.58^{+0.12}_{-0.14}$	8.30–8.83	8.17–8.96
δ/π (NO)	$1.08^{+0.13}_{-0.12}$	0.84–1.42	0.71–1.99
$\delta/^\circ$ (NO)	194^{+24}_{-22}	152–255	128–359
δ/π (IO)	$1.58^{+0.15}_{-0.16}$	1.26–1.85	1.11–1.96
$\delta/^\circ$ (IO)	284^{+26}_{-28}	226–332	200–353

5. RESULTS AND DISCUSSIONS

In this chapter we provide a summary of our results related to generating neutrino masses radiatively in the framework of the scotogenic model while respecting all the relevant constraints imposed on the parameter space of the model. We start first by showing the variation of the generated neutrino masses m_1, m_2 and m_3 with some of the chosen parameters of the scotogenic model. Here we show some results for illustration.

In our analysis we set $\theta_{12,23,13}$ and δ to their central values listed in table 4.1 for the normal ordering case of neutrino masses. Recall that the quantities listed in the table represent the recent fit to the global data on neutrino oscillations (P. F. de Salas, 2021). In the next step, we perform scanning over the related parameter space of the model which include the masses of $N_{1,2,3}, m_H, m_0$ and the parameters $Y_{1,2,3}$ contributing to the Yukaw couplings.

Regarding the scalar particles masses $m_{H^\pm}$, $m_{\mathcal{S}}$ and m_P, restrictions can be placed on the values using the data on W and Z widths in addition to the null results of direct searches for new particles at $e^+ e^-$ colliders. The constraints read $m_{H^\pm} + m_{\mathcal{S},\mathcal{P}} > m_{W^\pm}, m_{H^\pm} > 70\text{GeV}, m_{\mathcal{S}} + m_{\mathcal{P}} > m_Z$. On the other hand, concerning the new singlet fermion masses, the mass of N_1 is not constrained by current collider data and the masses of the fermions N_2 and N_3 have to be large to satisfy current lepton flavor violation. If we take into account the constraints from Dark Matter relic density and considering the scenario that N_1 plays the role of the Dark Matter candidate, one finds that for light dark matter masses $M_1 < 100$ GeV, lepton flavor violation (A. Vicente and C. E. Yaguna, 2015), and direct search at LHC(G. Aad et al. 2020),(A. M. Sirunyan et al. 2021), mostly exclude the parameter space of the model.

In Fig.5.1, we show the variation of m_1 with Y_1 for M_1=300 GeV and m_0=500 GeV. We find from the plot that m_1 increase with the increasing of Y_1.

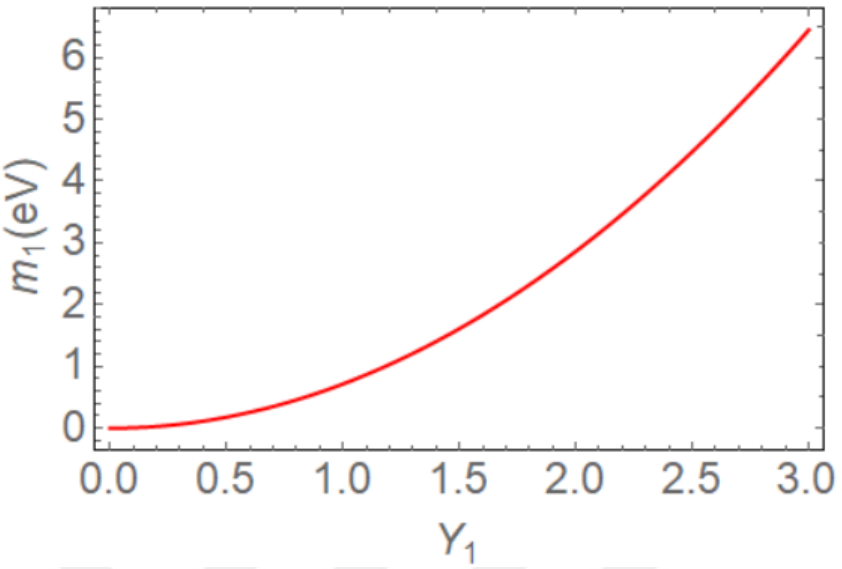

Figure 5.1. Variation of m_1 with Y_1 for M_1=300 GeV. m_0=500 GeV

In Fig.5.2. We show the variation of m_1 with m_0 for M_1=140 GeV and Y_1=2.1. We see from the figure that m_1 decreases with the increasing ofm_0.

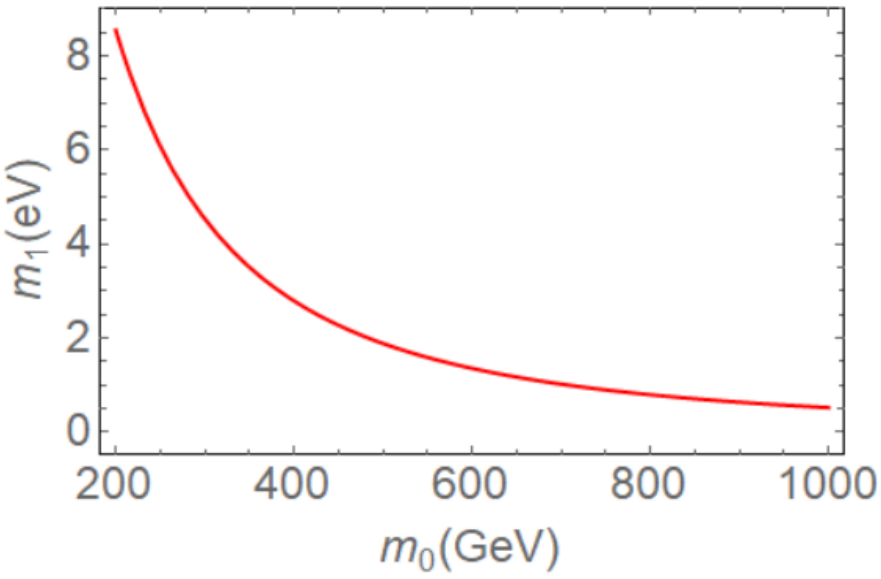

Figure 5.2. Variation of m_1 with m_0 for M_1=140 GeV and Y_1=2.1.

In Fig.5.3. We display the variation of m_1 with M_1 for m_0=500 GeV and Y_1=2.8. We deduce from the figure that $m_1$increases with the increasing of M_1.

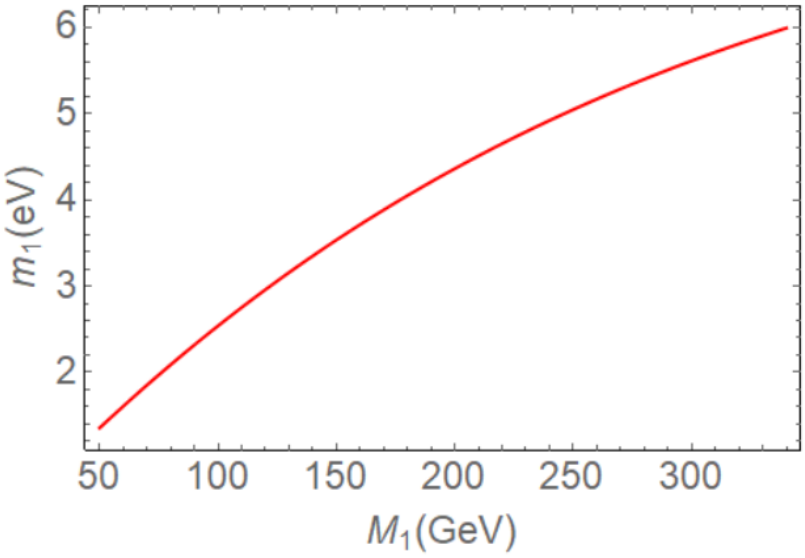

Figure 5.3. Variation of m_1 with M_1 for m_0 = 500 GeV and Y_1=2.8.

In Figs.5.4, we display our evaluation of the variation of m_2 with $M_2$and m_0 for Y_2=2.4.

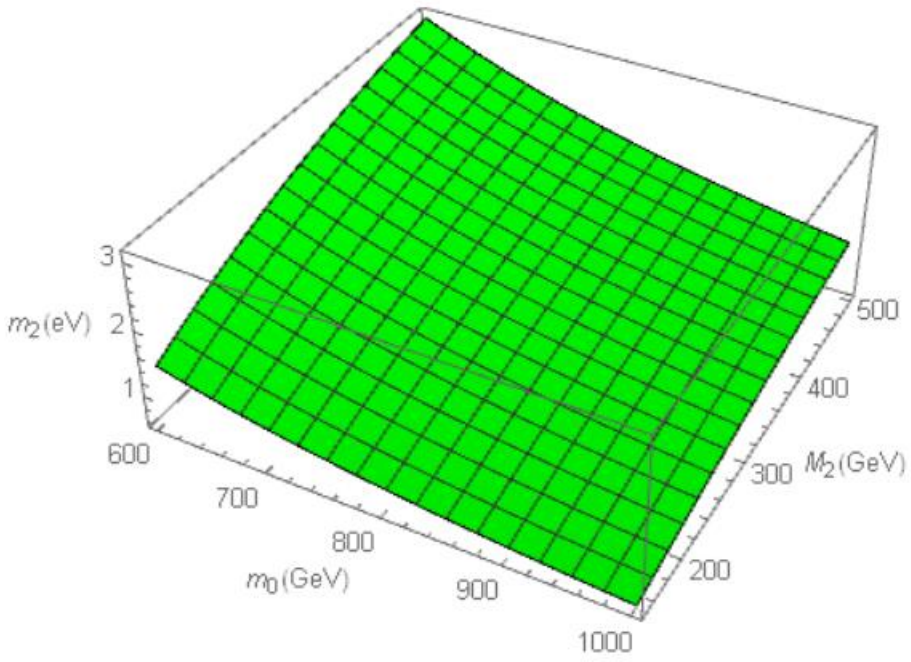

Figure 5.4. Variation of m_2 with M_2 and m_0 for Y_2=2.4.

From the figure one can deduce the generated mass m_2 for fixed values of M_2 and m_0.

In Figs.5.5, we display our results for the variation of m_2 with $M_2$and Y_2 for m_0=500 GeV. We deduce from the figure that $m_2$increases with the increasing of M_2. The figure shows that for m_0=500 GeV, it is possible for combinations of the parameters $M_2$and Y_2 to generate neutrino masses m_2 of order eV which is favored by experimental results.

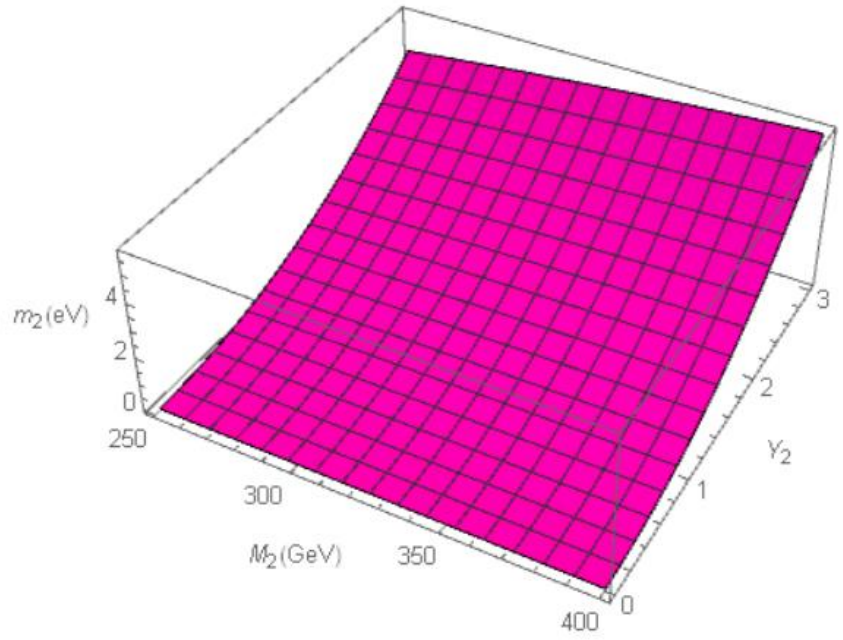

Figure 5.5. Variation of m_2 with M_2 and Y_2 for m_0=500 GeV .

In Figs.5.6, we display the variation of m_2 with m_0 and Y_2 for M_2=450 GeV. Similar conclusion can be made as discussed above but here we changed the parameters to m_0 and Y_2.

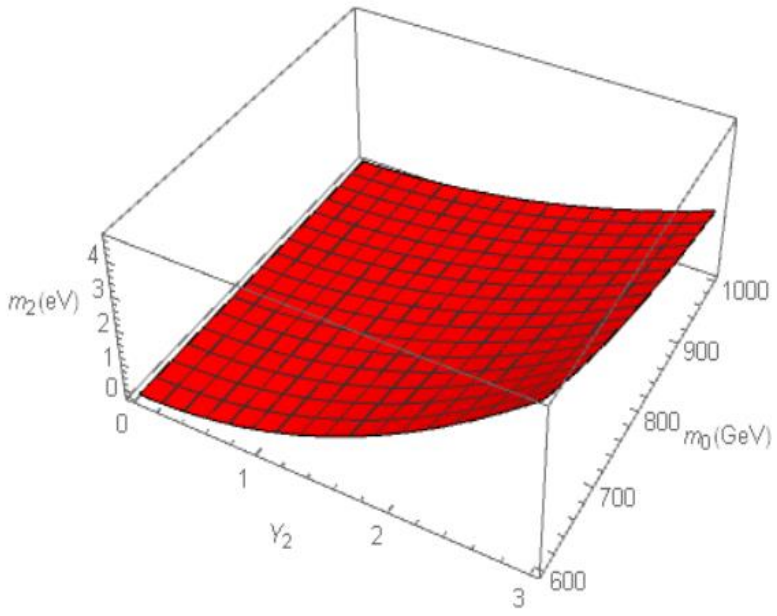

Figure 5.6. Variation of m_2 with Y_2 and m_0 for M_2=450 GeV.

In the following, we repeat the above analysis but here we concern about generating m_3 of the orders of eV. In Figs.5.7, we display the variation of m_3 with M_3 and m_0 for Y_3=0.3.

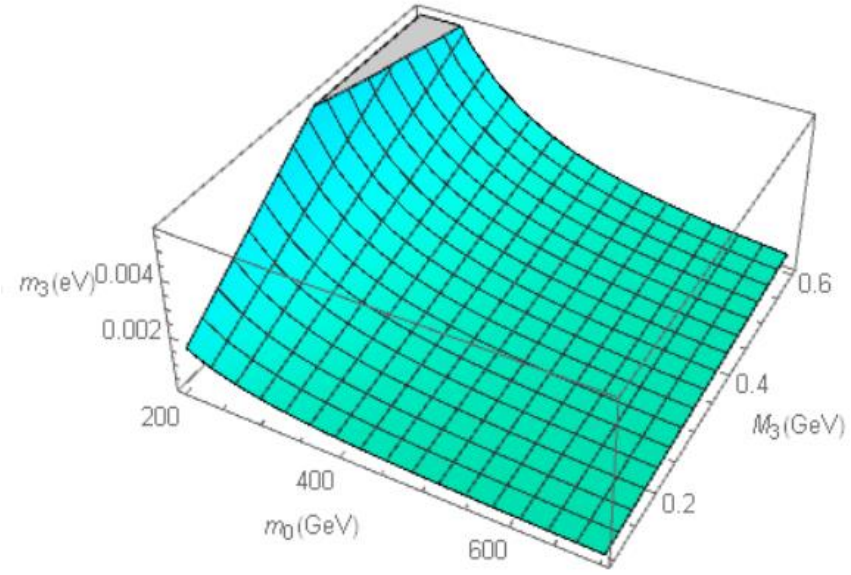

Figure 5.7. Variation of m_3 with M_3 and m_0 for Y_3=0.3

In Figs.5.8, we display the variation of m_3 with M_3 and Y_3 for m_0=700 GeV.

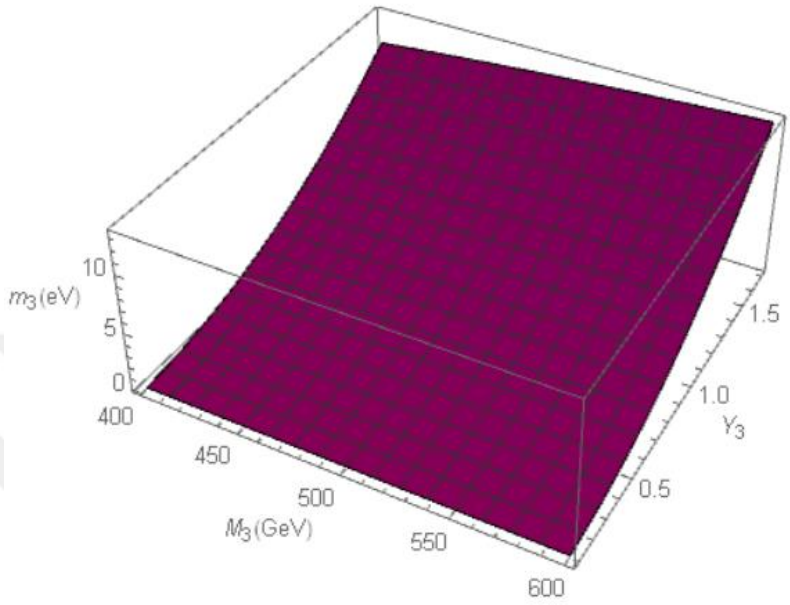

Figure 5.8. Variation of m_3 with M_3 and Y_3 for m_0=700 GeV .

In Figs.5.9, we display the variation of m_3 with m_0 and Y_3 for M_3=1000 GeV.

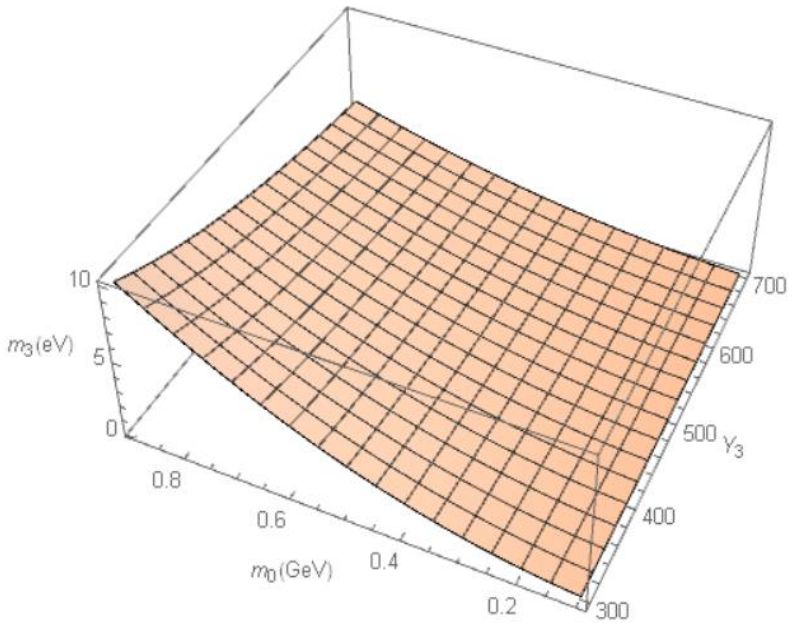

Figure 5.9. Variation of m_3 with Y_3 and m_0 for M_3=1000 GeV.

We deduce from Figs.5.7, Figs.5.8 and Figs.5.9 that there is parameter space in which the generated neutrino mass m_3 can be of orders eV which is favored by experimental searches.

In Fig.5.10. We show our results for the allowed regions in the $M_1 - Y_1$ plane 2σ Δm^2_{21} constraints listed in table 4.1 for a fixed value $Y_2 = 0.155$. The green, blue and red colors correspond to different m_H values. Here, we show the effect of variation of m_H on the allowed $M_1 - Y_1$ parameter space by Δm^2_{21} .

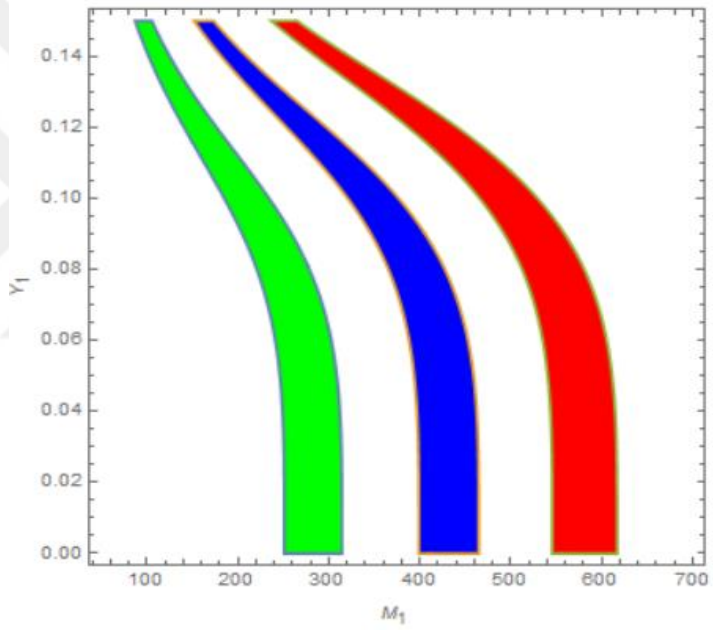

Figure 5.10. Allowed regions in the $M_1 - Y_1$ plane by 2σ range of Δm^2_{21} constraints for $M_2 = M_1 + 200$ GeV. The plot is obtained using $Y_2 = 0.155$ and the green, blue and red correspond to $m_H = M_1 + 300$ GeV, $m_H = M_1 + 400$ GeV and $m_H = M_1 + 500$ GeV respectively.

Clearly from Figure 5.10 that, varying the charged Higgs mass m_H has an effect on the allowed parameter space $M_1 - Y_1$ satisfying the 2σ range of Δm^2_{21} constraints. Additionally, from the same figure, large charged Higgs mass m_H permit large M_1 masses while small charged Higgs mass m_H allow small M_1 masses.

In Fig.5.11. We display the allowed regions in the $M_1 - Y_1$ plane by 2σ Δm^2_{21} constraints for $M_2 = M_1 + 200$GeV where we set $m_H = M_1 + 500$ GeV and the green, blue and red correspond to the values $Y_2 = 0.155$, $Y_2 = 0.165$ and $Y_2 = 0.175$ respectively.

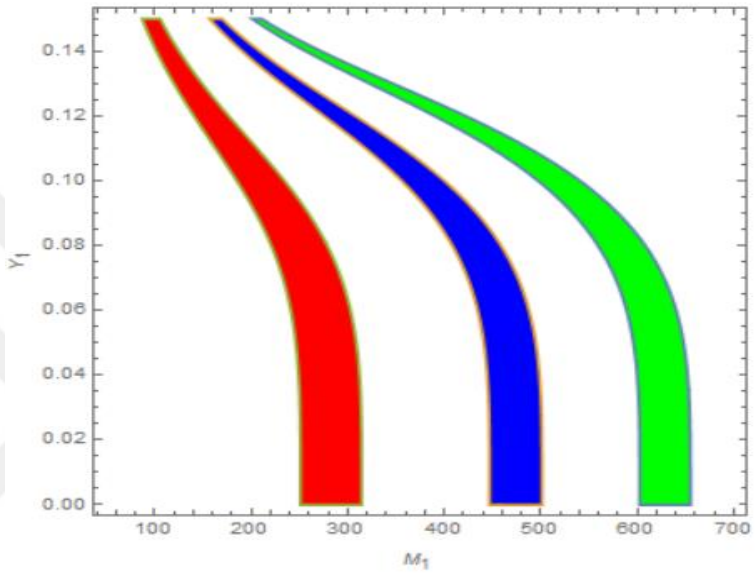

Figure 5.11. Allowed regions in the $M_1 - Y_1$ plane by 2σ range of Δm^2_{21} constraints for $M_2 = M_1 + 200$ GeV. In the r plot we set $m_H = M_1 + 500$ GeV and the green, blue and red correspond to the values $Y_2 = 0.155$, $Y_2 = 0.165$ and $Y_2 = 0.175$ respectively.

As can be seen from Figure 5.11, changing the Yukawa couplings Y_2 can affect the allowed parameter space $M_1 - Y_1$ satisfying the 2σ range of Δm^2_{21} constraints. Moreover, from the figure, large Yukawa couplings permit small M_1 masses while small Yukawa couplings allow large M_1 masses.

In Fig.5.12. We show our results for the allowed regions in the $M_1 - Y_1$ plane using the 2σ range of Δm^2_{31} constraints listed in table 4.1 and after setting $Y_2 = 0.5$, $M_2 = M_1 + 250$ GeV . The green plot is obtained for the parameters $m_H = M_1 + 700$ GeV while the blue plot is obtained for the parameters $m_H = M_1 + 600$ GeV and red plot is obtained for the parameters $m_H = M_1 + 500$ GeV.

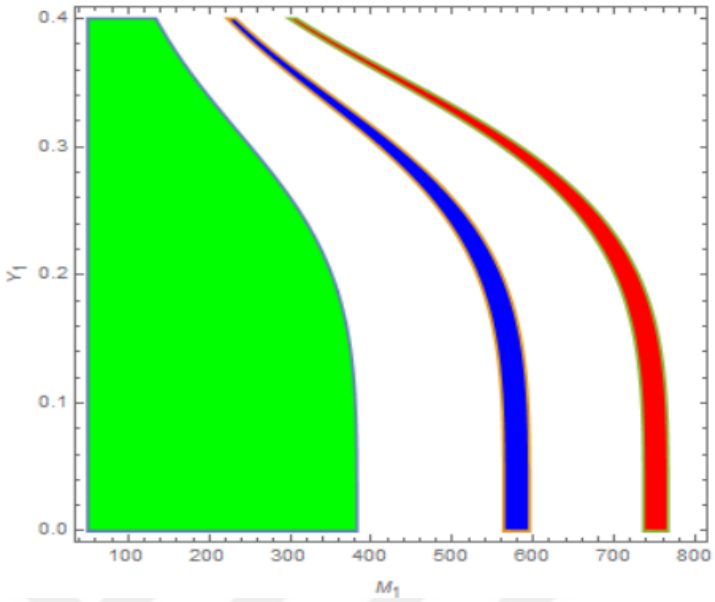

Figure 5.12. Allowed regions in the $M_1 - Y_1$ plane by 2σ range of Δm^2_{31} constraints. The plots are obtained using $Y_2 = 0.5$, $M_2 = M_1 + 250$ GeV. The green plot is obtained for the parameters $m_H = M_1 + 700$ GeV while the blue plot is obtained for the parameters $m_H = M_1 + 600$ GeV and the red plot is obtained for the parameters $m_H = M_1 + 500$ GeV.

Clearly from Figure 5.12 that, varying the charged Higgs mass m_H has an effect on the allowed parameter space $M_1 - Y_1$ satisfying the 2σ range of Δm^2_{31} constraints. Additionally, from the same figure we see that, large charged Higgs mass m_H permit small M_1 masses while small charged Higgs mass m_H allow large M_1 masses.

In Fig.5.13. We present our results for the allowed regions in the $M_1 - Y_1$ plane after considering the 2σ range of Δm^2_{31}. The plots are obtained after fixing the parameters as $m_H = M_1 + 500$ GeV, $M_2 = M_1 + 250$GeV. The green, blue and red plots corresponds to the Yukawa couplings $Y_2 = 0.4$, $Y_2 = 0.5$ and $Y_2 = 0.55$ respectively.

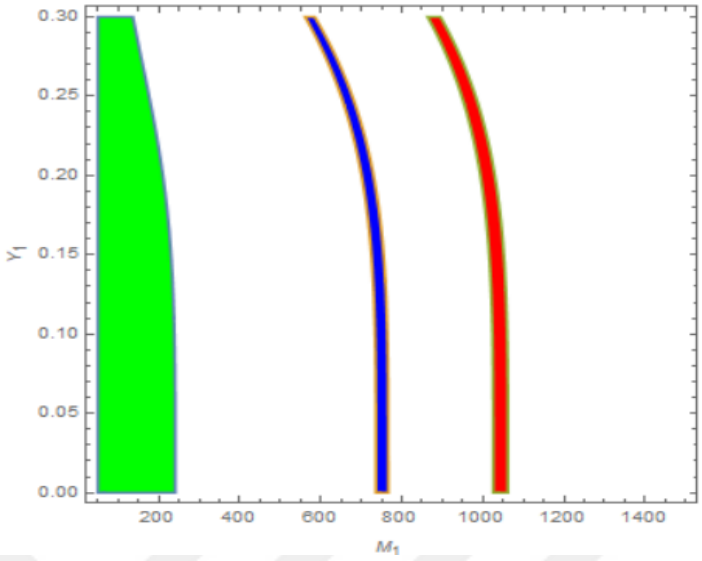

Figure 5.13. Allowed regions in the $M_1 - Y_1$ plane by 2σ range of Δm^2_{31} constraints. The plot is obtained for the parameters $m_H = M_1 + 500$ GeV, $M_2 = M_1 + 250$GeV. The green plot is obtained after taking $Y_2 = 0.4$, the blue plot corresponds to Y_2=0.5 and the red plot is obtained for the value Y_2=0.55.

As can be seen from Figure 5.13, changing the Yukawa couplings Y_2 can affect the allowed parameter space $M_1 - Y_1$ satisfying the 2σ range of Δm^2_{31} constraints. Moreover, from the figure, large Yukawa couplings permit large M_1 masses while small Yukawa couplings allow small M_1 masses.

We turn now to discuss the constraints imposed on the parameter space from the existing experimental limits on the LFV processes are$BR(\tau \to e\gamma)$, $BR(\tau \to \mu\gamma)$, and$BR(\mu \to e\gamma)$. In Figures 5.14, 5.15, 5.16, we show our results for the allowed regions in the $M_1 - Y_1$ plane by $BR(\tau \to e\gamma)$, $BR(\tau \to \mu\gamma)$, and BR ($\mu \to e\gamma$) constrain in green and red colors.

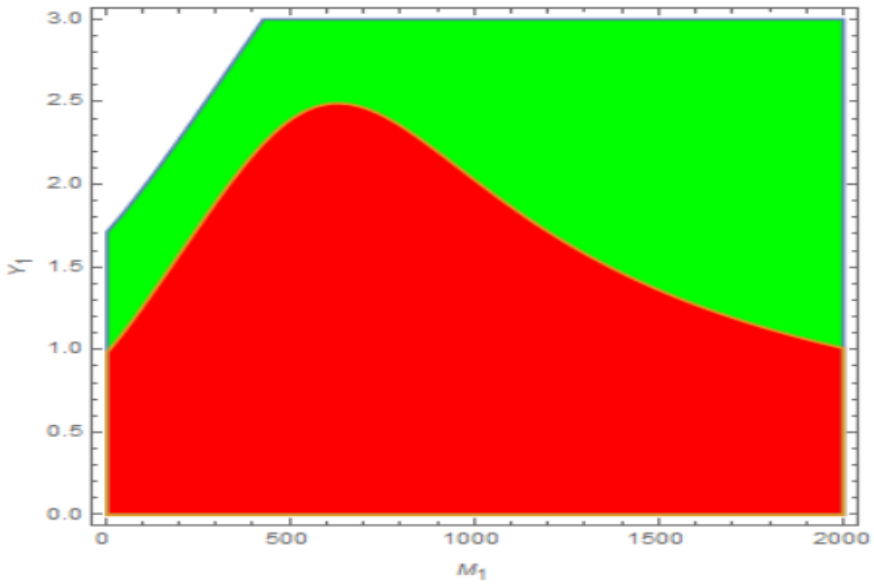

Figure 5.14. Allowed regions in the $M_1 - Y_1$ plane by$BR(\tau \to e\gamma)$, constraints. The plots are obtained usingY_2 =0.01, Y_3=0.03, M_2= M_1 + 200 GeV, M_3=M_1 + 250GeV. The green color corresponds to the value $m_H = M_1 + 700$ GeV while the red plot is obtained for the parameter $m_H = M_1 + 400$ GeV.

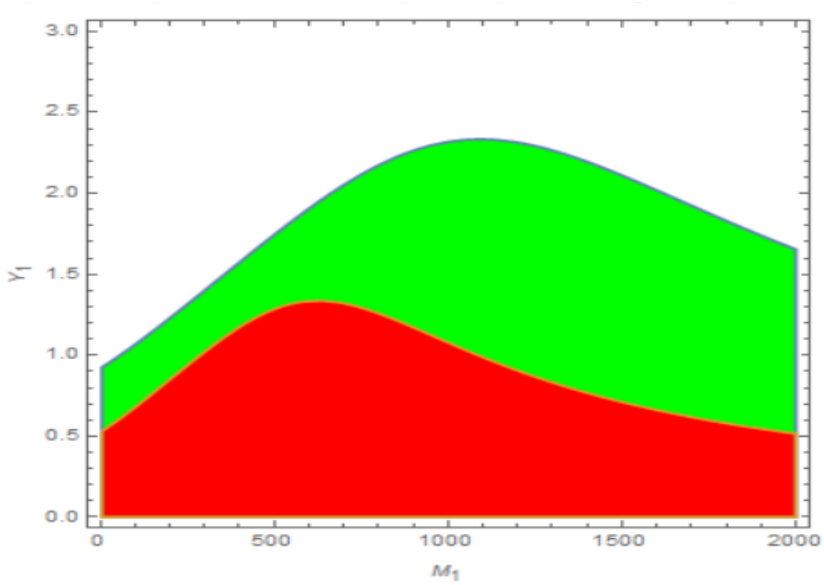

Figure 5.15. Allowed regions in the $M_1 - Y_1$ plane $BR(\tau \to \mu\gamma)$, constraints. The plots are obtained usingY_2 =0.01, Y_3=0.03, M_2= M_1 + 200 GeV, M_3=M_1 + 250 GeV. The green plot is obtained for the parameters $m_H = M_1 + 700$ while the red plot is obtained for the parameters $m_H = M_1 + 400$ GeV.

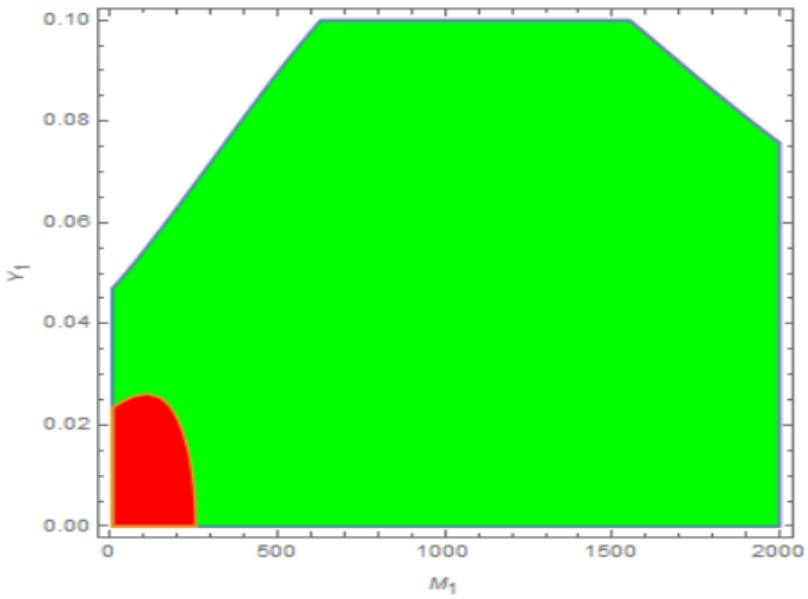

Figure 5.16. Allowed regions in the $M_1 - Y_1$ plane by$BR(\mu \to e\gamma)$ constraints. The plots are obtained usingY_2 =0.01, Y_3=0.03, M_2= M_1 + 200 GeV, M_3=M_1 + 250 GeV. The green color corresponds to a value m_H = M_1 + 700 G while the red plot is obtained for the parameters m_H = M_1 + 400 GeV.

We remark from Figures 5.14, 5.15, 5.16 that, for large m_H value the coupling Y_1 can be large compared to the case of having small m_H value in all plots. In addition, we note from the plot that the weakest constraints $BR(\tau \to e\gamma)$ and the strongest constraints is $BR(\mu \to e\gamma)$.

In Fig.5.17. We show our results for the allowed regions in the $Y_1 - Y_2$ plane by the summation of neutrino masses $\sum m_i < 0.12$eV where we fixed the other parameters as , m_0 = 600 GeV, M_1=200 GeV, M_2=200 GeV, M_3=200 GeV and Y_3=0.12. Clearly from the figure that one cannot choose large values for both Y_1 and Y_2 large at the same time as picking them large will not respect the constraint.

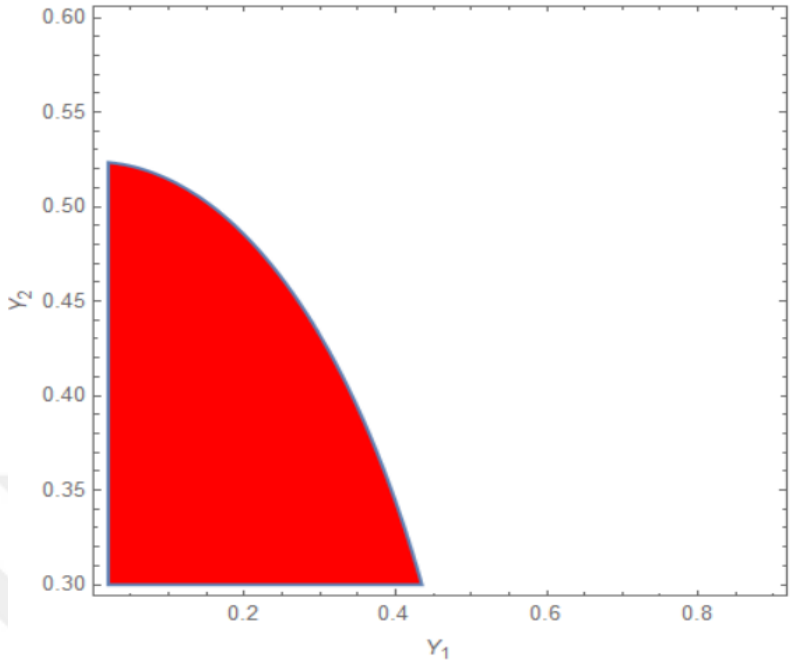

Figure 5.17. Allowed region in the $Y_1 - Y_2$ plan m_0 =600 GeV , M_2= 200 GeV, M_3=200 GeV and Y_3=0.12

Having discussed the most important constraints on the parameter space of the scotogenic model, it is important to check if there is possibility to generate the small neutrino masses and finding a candidate for Dark matter whole respecting the dominant constraints imposed on the model. We have found that if we choose the case in which N_1 and N_2 have amost nearly equal masses they can play the role of dark matter candidate and satisfy the constraints from the relic density. In Fig.5.18. We show our results for the allowed regions in the $M_1 - Y_1$ plane by the dominant constraints $\mu \to e\gamma$, $\frac{|\Delta m^2_{31}|}{\Delta m^2_{21}}$, and $\Omega\hat{h}^2$constraints in red, blue, and magenta colors, respectively, corresponding to the NO scenario for Y2 = 0.49 and Y3 = 0.66 Y2 = 0.55 and Y3 =0.6. The intersection region of the three colors represents the allowed region by all constraints. That is to say, the region in which light neutrino masses can be generated and respecting the allowed values in Table 4.1 and also produce the measured value of relic density where N_1 and N_2 play the role of Dark Matter candidate.

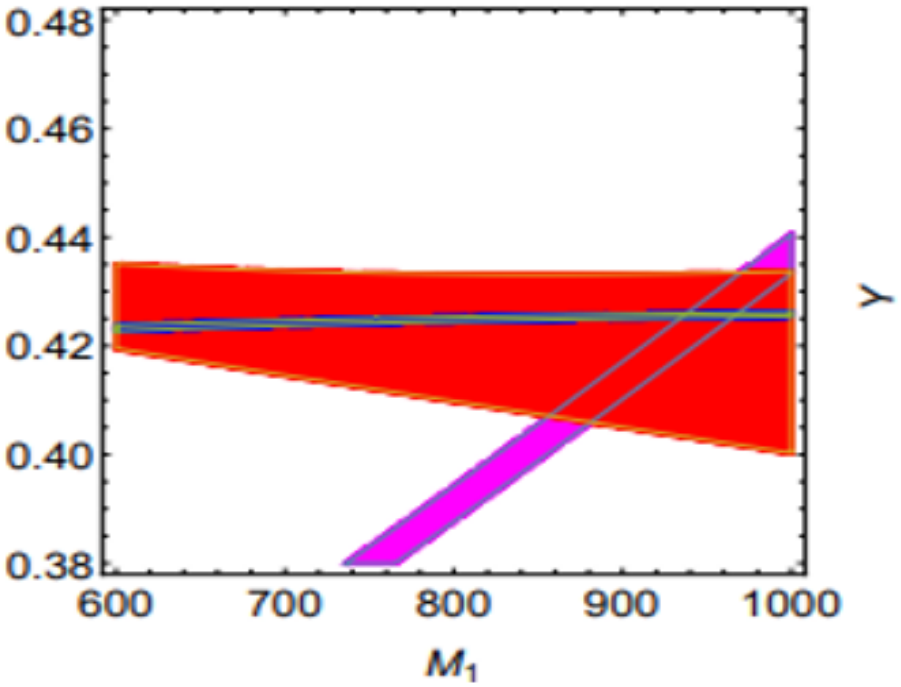

Figure 5.18. Allowed regions in the $M_1 - Y_1$ plane in red, blue, and magenta colors, respectively, corresponding to NO scenario for Y2 = 0.49 and Y3 = 0.66

6. CONCLUSIONS

One of the drawbacks of the standard model is the absence of mechanism for generating neutrino masses. This is attributed to the fact that neutrinos are left-handed in the standard model. Thus, neutrinos cannot have Dirac masses that requires the presence of both left and right handed components which are the cases in quarks and charged leptons. In the standard model also neutrinos do not couple with Higgs field responsible for generating masses of quarks and charged leptons. The absence of mechanism for generating neutrino masses can be a hint for new physics beyond the standard model.

In this thesis we have explored one of the possible new physics beyond the standard model of particle physics namely, the scotogenic model. In this model, neutrino masses can be generated radiatively through a one loop Feynman diagram with new particles associated with the model running in the loop. These new particles are the three singlet right handed fermions N_1, N_2 and N_3 and the scalar and pseudoscalar components of the extra Higgs doublet proposed in the scotogenic model.

In our study carrıed out in this thesis, we investigated the parameter space of the scotogenic model that can lead to generation of neutrino masses of order eV which are favored by several experimental results related to neutrino mixing and oscillations. We showed that this is possible for some ranges in the parameter space of the model without violating the bounds obtained from several processes such as lepton flavor process, relic density measurements and other relevant bounds discussed in details in the text before.

With this result in hand, it is interesting to check the model predictions for specific processes that can be tested in current and future colliders for the obtained parameter space. Doing so and compare the results with the standard model and scotogenic model predictions of such processes can shed light on new physics beyond standard model.

REFERENCES

A. Ahriche and S. Nasri, JCAP 1307, 035, 2013.

A. Heister et al. [ALEPH Collaboration], Eur. Phys. J. C 38, 147 ,2004 ; J. Abdallah et al. [DELPHI Collaboration], Eur. Phys. J. C 34, 127, 2004; P. Achard et al. [L3 Collaboration], Phys. Lett. B 600, 22 (2004); G. Abbiendi et al. [OPAL Collaboration], Eur. Phys. J. C 52, 767, 2007.

A. M. Sirunyan et al. [CMS], JHEP 04, 123,2021.

A. M. Baldini et al. [MEG], Eur. Phys. J. C 76, no.8, 434,2016.

A. Vicente and C. E. Yaguna, JHEP 02, 144, 2015.

A. Zee, A Theory of Lepton Number Violation, Neutrino Majorana Mass, and Oscillation, Phys. Lett. B93, 389 , 1980.

Bouchand, Romain ,2012. Radiative Neutrino Mass Generation and Renormalization Group Running in the Ma-Model [Master's thesis, Royal Institute of Technology, SE-106 91 Stockholm, Sweden].

B. Pontecorvo, Mesonium and anti-mesonium, Sov. Phys. JETP 6 ,1957, 429.

B. Pontecorvo, Neutrino Experiments and the Problem of Conservation of Leptonic Charge, Zh. Eksp. Teor. Fiz. 53, 1967, 1717-1725.

B. Aubert et al. [BaBar], Phys. Rev. Lett. 104, 021802,,2010.

B. Pontecorvo, Sov. Phys. JETP 26, 1968, 984 [Zh. Eksp. Teor. Fiz. 53,1968, 1717]; Z. Maki, M. Nakagawa, and S. Sakata, Prog. Theor. Phys. 28, 870,1962.

C. Boehm, Y. Farzan, T. Hambye, S. Palomares-Ruiz, and S. Pascoli, Phys. Rev. D 77, 043516, 2008; Y. Farzan, Phys. Rev. D 80, 073009 , 2009; Mod. Phys. Lett. A 25, 2111, 2010.

C. Jarlskog, Commutator of the Quark Mass Matrices in the Standard Electroweak Model and a Measure of Maximal CP Violation, Phys. Rev. Lett. 55, 1985, 1039.

D. Buskulic et al. [ALEPH Collaboration], Phys. Lett. B 384, 333, 1996; R. Barate et al. [ALEPH Collaboration], Phys. Lett. B 420, 127 [arXiv:hep-ex/9710009]; R. Barate et al. [ALEPH Collaboration], Phys. Lett. B 429, 201, 1998; A. Heister et al. [ALEPH Collaboration], Eur. Phys. J. C 28, 1, 2003; P. Abreu et al. [DELPHI Collaboration], Eur. Phys. J. C 17, 53, 2000 [arXiv:hep ex/0103044]; J. Abdallah et al. [DELPHI Collaboration], Eur. Phys. J. C 38, 395, 2005 M. Acciarri et al. [L3 Collaboration], Phys. Lett. B 415, 299, 1997; M. Acciarri et al. [L3 Collaboration], Phys. Lett. B 444, 503 1998; M. Acciarri et al. [L3 Collaboration], Phys. Lett. B 470, 268,1999 [arXiv:hep-ex/9910009]; K.

Ackerstaff et al. [OPAL Collaboration], Eur. Phys. J. C 2, 607, 1998 [arXiv:hep-ex/9801024]; G. Abbiendi et al. [OPAL Collaboration], Eur. Phys. J. C 8, 23, 1999; G. Abbiendi et al. [OPAL Collaboration], Eur. Phys. J. C 18, 253, 2000.

D. Suematsu, T. Toma, and T. Yoshida, "Enhancement of the annihilation of dark matter in a radiative seesaw model," Phys. Rev. D 82, 013012, 2010.

E. K. Akhmedov, Do charged leptons oscillate?, JHEP 09, 2007, 116 [arXiv:0706.1216 [hep-ph]].

E. Ma, Phys. Rev. D 73, 077301, 2006 [hep-ph/0601225].

E. Ma and M. Raidal, Phys. Rev. Lett. 87, 011802, 2001 [Erratum-ibid. 87, 159901, 2001].

F. R. Klinkhamer and N. S. Manton, A saddle-point solution in the Weinberg Salam theory, Phys. Rev. D30, 2212, 1984.

F.P. An et al. [DAYA-BAY Collaboration], Phys. Rev. Lett. 108, 171803, 2012 [arXiv:1203.1669 [hepex]]; J.K. Ahn et al. [RENO Collaboration], Phys. Rev. Lett. 108, 191802, 2012 [arXiv:1204.0626 [hep-ex]].

G. Aad et al. [ATLAS Collaboration], Phys. Lett. B 716, 1, 2012 [arXiv:1207.7214 [hep-ex]]; S. Chatrchyan et al. [CMS Collaboration], Phys. Lett. B 716, 30, 2012 .

G. Aad et al. [ATLAS], Phys. Rev. D 101, no.5, 052005, 2020.

G. B. Gelmini and M. Roncadelli, Left-Handed Neutrino Mass Scale and Spontaneously Broken Lepton Number, Phys. Lett. B99, 411, 1981.

G. Faisel, S. Y. Ho, and J. Tandean, "Exploring X-Ray Lines as Scotogenic Signals," Phys. Lett. B 738, 380–385, 2014.

G. Guo, X.G. He, and G.N. Li, JHEP 1210, 044, 2012 [arXiv:1207.6308 [hep-ph]]; G.N. Li, G. Guo, B. Ren, Y.J. Zheng, and X.G. He, JHEP 1304, 026, 2013 [arXiv:1212.5528 [hep-ph]].

J. Beringer et al. [Particle Data Group Collaboration], Phys. Rev. D 86, 010001, 2012.

J. Kubo, E. Ma, and D. Suematsu, Phys. Lett. B 642, 18, 2006 [hep-ph/0604114]; D. Suematsu, T. Toma, and T. Yoshida, Phys. Rev. D 79, 093004, 2009 [arXiv:0903.0287 [hep-ph]]; D. Schmidt, T. Schwetz, and T. Toma, Phys. Rev. D 85, 073009, 2012 [arXiv:1201.0906 [hep-ph]].

JHEP \textbf{02}, 071, 2021 doi:10.1007/JHEP02, 2021, 071 [arXiv:2006.11237 [hep-ph]].

J. Liu, Z. L. Han, Y. Jin and H. Li, Unraveling the Scotogenic model at muon collider, JHEP 12, 057, 2022 ,doi:10.1007/JHEP12, 2022, 057.

J.I.Illana and A.Jimenez Cano,Quantum field theory and the structure of the Standard Model,PoS \textbf{CORFU2021}, 314 , 2022, doi:10.22323/1.406.0314.

K. S. Babu and E. Ma, Natural Hierarchy of Radiatively Induced Majorana Neutrino Masses, Phys. Rev. Lett. 61, 674, 1988.

K. S. Babu, Model of 'calculable' Majorana neutrino masses, Phys. Lett. B203, 132, 1988.

M. Gell-Mann, P. Ramond and R. Slansky, Complex Spinors and Unified Theories, Conf. Proc. C 790927, 1979, 315-321 [arXiv:1306.4669 [hep-th]].

M. Kobayashi and T. Maskawa, CP Violation in the Renormalizable Theory of Weak Interaction, Prog. Theor. Phys. 49,1973, 652-657.

M. Schwartz, Quantum Field Theory and the Standard Model, Cambridge University Press, 2014.

M.C. Gonzalez-Garcia, M. Maltoni, J. Salvado, and T. Schwetz, JHEP 1212, 123, 2012 [arXiv:1209.3023 [hep-ph]].

N. Cabibbo, Unitary Symmetry and Leptonic Decays, Phys. Rev. Lett. 10,1963, 531-533.

P. A. Zyla et al. [Particle Data Group], Review of Particle Physics, PTEP, 2020 no.8, 083C01.

P. F. de Salas, D. V. Forero, S. Gariazzo, P. Mart´ınez-Mirave,´ O. Mena, C. A. Ternes, M. Tortola and J. W. F. Valle, JHEP ´ 02, 071,2021.

P. F. de Salas, D. V. Forero, S. Gariazzo, P. Martínez-Miravé, O. Mena, C. A. Ternes, M. Tórtola and J. W. F. Valle, 2020 global reassessment of the neutrino oscillation picture, JHEP 02, 2021, 071 [arXiv:2006.11237 [hep-ph]].

P.A.R. Ade et al. [Planck Collaboration], arXiv:1303.5062 [astro-ph.CO].

P.F.de Salas, D.V.Forero, S.Gariazzo, P.Mart\nez-Mirav\'e, O.Mena, C.A.Ternes, M.T\'ortola and J.W.F.Valle, 2020 global reassessment of the neutrino oscillation picture, JHEP 02, 071, 2021 doi:10.1007/JHEP02, 2021, 071

Phys. Lett. B 47, 1973, 365-368.

R. N. Mohapatra and G. Senjanovi´c, Neutrino Mass and Spontaneous Parity Nonconservation, Phys. Rev. Lett. 44, 912, 1980.

R. N. Mohapatra and G. Senjanovi´c, Neutrino Mass and Spontaneous Parity Nonconservation, Phys. Rev. Lett. 44, 912, 1980.

R. N. Mohapatra and P. B. Pal, Massive neutrinos in physics and astrophysics. Second edition, World Sci. Lect. Notes Phys. 60, 1998, 1-397; 72, 1, 2004.

S. L. Glashow, J. Iliopoulos and L. Maiani, Weak Interactions with Lepton-Hadron Symmetry, Phys. Rev. D 2, 1970, 1285-1292.

S. L. Glashow, Partial Symmetries of Weak Interactions, Nucl. Phys. 22, 1961, 579-588.

S. Y. Ho and J. Tandean, "Probing Scotogenic Effects in Higgs Boson Decays," Phys. Rev. D 87, 095015 (2013).

S.Y. Ho and J. Tandean, Phys. Rev. D 87, 095015, 2013 [arXiv:1303.5700 [hep-ph]].

T. Behnke et al., arXiv:1306.6327 [physics.acc-ph].

T. Hambye, Phenomenology of the type iii seesaw model, 2009.

T. Kitabayashi, "Primordial black holes and lepton flavor violation with scotogenic dark matter," PTEP 2022, no.3, 033B02, 2022 .

T. Kitabayashi, Int. J. Mod. Phys. A 36, 2150139 (2021)

T. Yanagida, Horizontal gauge symmetry and masses of neutrinos, Conf. Proc. C 7902131, 1979, 95-99.

The one-loop renormalization of this model has been investigated in R. Bouchand and A. Merle, JHEP 1207, 084, 2012 [arXiv:1205.0008 [hep-ph]].

T. Toma and A. Vicente, JHEP 01, 160, 2014.

V. Kuzmin, V. Rubakov and M. Shaposhnikov, On anomalous electroweak baryon-number non-conservation in the early universe, Phys. Lett. B155, 36, 1985.

W. of Ockham, Quaestiones et decisiones in quattuor libros Sententiarum Petri Lombardi ed. Lugd.1495.

X. G. He, Is the Zee model neutrino mass matrix ruled out, Eur. Phys. J. C34, 371, 2004, hep-ph/0307172.

Z. Maki, M. Nakagawa and S. Sakata, Remarks on the unified model of elementary particles, Prog. Theor. Phys. 28, 1962, 870-880.